Transportation Research Part B 99 (2017) 113–137

Contents lists available at ScienceDirect

Transportation Research Part B

journal homepage: www.elsevier.com/locate/trb

Joint optimal train regulation and passenger flow control strategy for high-frequency metro lines

Shukai Li[a,*], Maged M. Dessouky[b], Lixing Yang[a], Ziyou Gao[a]

[a] State Key Laboratory of Rail Traffic Control and Safety, Beijing Jiaotong University, Beijing, 100044, China
[b] The Daniel J. Epstein Department of Industrial and Systems Engineering, University of Southern California, Los Angeles, CA 90089-0193, USA

ARTICLE INFO

Article history:
Received 13 September 2016
Revised 19 January 2017
Accepted 20 January 2017

Keywords:
Train regulation
Passenger flow control
Quadratic programming
System stability

ABSTRACT

To improve the headway regularity and commercial speed of high-frequency metro lines with overloaded passenger flow, this paper systematically investigates a joint optimal dynamic train regulation and passenger flow control design for metro lines. A coupled state-space model for the evolution of the departure time and the passenger load of each train at each station is explicitly developed. The dwell time of the train is affected by the number of entering and exiting passengers. Combining dynamic train regulation and passenger flow control, a dynamic optimisation problem that minimises the timetable and the headway deviations for metro lines is developed. By applying a model predictive control (MPC) method, we formulate the problem of finding the optimal joint train regulation and passenger flow control strategy as the problem of solving a set of quadratic programming (QP) problems, under which an optimal control law can be numerically calculated efficiently using a quadratic programming algorithm. Moreover, based on the Lyapunov stability theory, the stability (convergence) of the metro line system under the proposed optimal control algorithm is verified. Numerical examples are given to illustrate the effectiveness of the proposed method.

1. Introduction

1.1. Motivation

Urban metro transportation systems have became a rapid, clean, efficient way to transport passengers in many modern large cities for relieving the traffic pressure. Different to traditional passenger railway traffic, metro line systems have inherent features of high frequency and traffic density, which can lead to instability of this transportation system. Any deviation with respect to the nominal schedule of a given train is amplified with time due to the accumulation of passengers, which is similar to the familiar bus bunching problem in which the accumulation of passengers also leads to the instability of the bus system (Daganzo, 2009; Daganzo and Pilachowski, 2011; Sánchez-Martínez et al., 2016). If an inevitable disturbance happens on the metro line system, such as equipment failure or inadequate driver/passenger actions, the train will be delayed and train delays will increase from one station to the next with the accumulation of passengers, so that the whole metro line system operation will be affected. In order to restore the disturbed traffic to an acceptable situation for metro lines, train

* Corresponding author.
E-mail addresses: shkli@bjtu.edu.cn (S. Li), lxyang@bjtu.edu.cn (L. Yang).

http://dx.doi.org/10.1016/j.trb.2017.01.010

regulation manipulating the running time and the dwell time of each train is therefore necessary to recover train delays and to prevent the instability of the metro line operation.

With increasing urbanization, the increasing population and economic activities create a significant rise for the demand of metro transportation systems. Typically, the passenger arrival flow is extremely large during the peak hours of the workday. For example, a survey of the Beijing metro line system shows that the overloaded passenger count of the trains usually exceeds 120% during peak hours, causing a number of stations to adopt measures to control the passenger arrival flow. The dwell time of the train at the station depends on the number of passengers arriving to the station. The high passenger arrival flow during the peak hours magnifies the dwell time of the train and leads to train delays, especially under the case of a disturbance event occurring. The overloaded passenger flow aggravates the instability of metro lines and further affects the operational efficiency of the metro lines. Therefore, for the peak hours of the workday, it is essential to investigate how to control the large passenger arrival rate, apart from conducting train regulation to recover train delays from disturbed situations.

Since metro-type rail lines operate according to a given timetable, the main goal of regulation is a full timetable recovery to improve the commercial speed (the total travelling speed), while maintaining the regularity of the headway to minimize the accumulation of passengers and reduce undue passenger waiting time (Fernandez et al., 2006). The regulation of metro lines seeks a compromise between timetable and headway deviations during the transient period. Based on this, the research scope of this paper is a full timetable recovery from train delays under disturbances in a certain range, and the aim is to determine the joint dynamic train regulation and passenger flow control strategy by taking into consideration the overloaded passenger flow, providing the system with flexibility for recovery from disturbed situations, so as to ensure the stability and improve the headway regularity and commercial speed of the metro line system.

1.2. Literature review

As an important transportation mode in a modern metropolis, the metro line system has attracted substantial attention by researchers over the last decades. The literature on the metro line system includes two main categories: train timetabling (train schedules) and train rescheduling problems. The train timetabling problem aims to determine a pre-operation schedule for a set of trains for the metro line system, while the target of the train rescheduling process is to cope with the unpredicted events and the train rescheduling model needs to adjust the current timetable in an effective way when a disturbance occurs.

To study the train timetabling problem of a metro line system, the early work of Cury et al. (1980) proposed an analytical model with two dynamic equations: the headway and the passenger equations, and established a cost function that includes passenger delay, passenger comfort, and efficient train operation. The generation of optimal schedules for metro lines was formulated as a nonlinear dynamic programming problem, and solved by an iterative hierarchical multilevel decomposition method. Minciardi et al. (1995) dealt with the problem of generating daily train schedules for an underground railway line, which optimized the quality of the service expressed as the mean time spent by the passengers in the system with the safety constraints on the motion of trains. To improve the computational efficiency, Assis and Milani (2004) proposed a new methodology for computing the optimal train schedules for metro lines using a linear-programming-based model predictive control formulation. The proposed methodology is computationally efficient and can generate optimal schedules for a whole day operation as well as schedules for transitions between two separate time periods with known schedules. Mannino and Mascis (2009) discussed a number of theoretical and practical results related to the implementation of an exact algorithm to route and schedule trains in real time for metro stations. Niu and Zhou (2013) focused on optimizing a passenger train timetable in a heavily congested urban rail corridor, and developed a nonlinear optimization model to solve the problem on practical sized corridors subject to the available train-unit fleet. Sun et al. (2014) formulated three optimization models to design demand-sensitive timetables for metro services by representing train operations using equivalent time. Li and Hong (2014) formulated an integrated energy-efficient operation model to optimize the timetable and speed profile for metro line operations. Niu et al. (2015) developed train schedules to minimize the total passenger waiting time using a nonlinear integer programming model with linear constraints. Yang et al. (2016) developed a two-stage stochastic integer programming model to minimize the expected travel time and penalty value incurred by transfer activities for metro networks. Das Gupta et al. (2016) proposed a two-step linear optimization model to calculate energy-efficient timetables for metro railway networks. Yin et al. (2017) designed a dynamic passenger demand oriented metro train scheduling to minimize the energy consumption and waiting time by using a mixed-integer linear programming approach.

In case a disturbance or a disruption occurs in the metro line, the optimized train timetables are not able to keep the original optimized objectives. The train rescheduling process has to be initiated to recover train delays and reduce the effect of the unpredicted events (Chang and Chung, 2005; Corman et al., 2012; Dundar and Sahin, 2013; Cacchiani et al., 2014; Veelenturf et al., 2016). Usually, for the general railway system with the larger travel time, the train operation strategies, such as overtaking, meeting and crossing are allowable to implement for improving rescheduling efficiency. However, these strategies are commonly prohibited in an urban metro system with the smaller travel time, where the trains have the same priority, and the overtaking between train is not allowed for metro lines (Van Breusegem et al., 1991; Niu et al., 2015; Yin et al., 2016). In addition, the metro train rescheduling should particularly consider the passengers' influencing factors (Van Breusegem et al., 1991; Yin et al., 2016). The methods for the general railway rescheduling are usually infeasible for metro train rescheduling problems.

In particular, there are two rescheduling approaches for an urban metro system, where one is to recover the original timetable, and another is to redesign a new train scheduling plan. Every day small or slight delays occur in almost all the urban metro lines, and the affected trains need several stations to compensate for the delays, then a transient period is needed to reach the nominal timetable. In this case, the train regulation strategy by dynamically adjusting the running time and the dwell time of each train is applied to recover the original timetable from disturbances (Fernandez et al., 2006; Lin and Sheu, 2010). The corresponding train rescheduling is also called Automatic Train Regulation (ATR), which is a core function of modern metro signalling systems and plays an important role in maintaining schedule and headway adherence. The train regulation strategy is an on-line and dynamic rescheduling approach, which is based on real-time feedback information and generates the train rescheduling strategy in real-time. On the other hand, in the presence of large delays, if the duration of the regulation transient and the magnitude of time deviations from the nominal timetable are unacceptable, then a rescheduling process is needed, and a new delayed nominal timetable could be established, which is an off-line rescheduling approach with the real-time requirement for the algorithm design (Corman et al., 2012; Dundar and Sahin, 2013; Yin et al., 2016). For the above two rescheduling approaches, this paper focuses on the first case to recover the original timetable from disturbances.

Usually, the buffer times or supplements in the timetable are designed to absorb the train delays resulting from disturbances (Vansteenwegen and Oudheusden, 2004; Abril et al., 2008). However, buffer time allocations are static and cannot be used dynamically and flexibly from a system-wide point of view, which may reduce the system utilization. Moreover, on-line train regulation can be applied to recover the schedule/headway deviations resulting from disturbances by dynamically adjusting the running time and the dwell time of each train. Many online train regulation techniques have been proposed for metro lines. Van Breusegem et al. (1991) proposed a complete discrete-event traffic model of metro lines and designed a state feedback control algorithm to ensure system stability and the minimization of a given performance index based on a linear quadratic regulator approach. This model is useful to analyze the stability of a metro-type traffic regulation. By using a fuzzy expert system approach, Chang and Thia (1996) designed an online timetable rescheduling of mass rapid transit trains to maintain the quality of train service after sudden load disturbances. The proposed methodology is fast enough for online implementation. Goodman and Murata (2001) proposed a classical optimization approach to regulating metro traffic to encapsulate the travelling passengers perception of the quality of the service provided. In Chang and Chung (2005), a genetic algorithm was applied to solve the optimal train regulation problem efficiently. Fernandez et al. (2006) proposed a predictive traffic regulation model for metro loop lines on the basis of the optimization of a cost function along a time horizon and proposed regulation strategies to minimize the timetable and headway deviations by modifying the train run times. Lin and Sheu (2010) proposed an automatic train regulation method using a dual heuristic dynamic program to handle the nonlinear and stochastic characteristics of metro lines, and obtained a near-optimal regulation rapidly. Recently, regarding environment sustainability and energy saving, Sheu and Lin (2012) proposed a dual heuristic programming method for designing automatic train regulation of a metro line with energy saving by coasting and station dwell time control, and the evaluation shows that better traffic regulation with higher energy efficiency is attainable. Kang et al. (2015) proposed a rescheduling model for the last train by considering the train delays caused by incidents that occurred in urban railway transit networks, and designed a genetic algorithm to minimize the difference between the original timetable and the rescheduled one. Xu et al. (2016) considered an incident on a track of a double-track subway line, and formulated an optimization model to find near-optimal rescheduled timetables with the least total delay time compared to the original one.

Train regulation problems for metro lines are usually formulated as an optimization problem and solved using nonlinear programming or dynamic programming by combining heuristic algorithms. However, for large-scale nonlinear optimization problems, the computation time is still long, making the problem intractable in real time. In this paper, we use a model predictive control (MPC) algorithm to efficiently handle large-scale optimization problems with hard physical constraints, which have been successfully applied in many large-scale transportation systems (Caimi et al., 2007; Le et al., 2013). For instance, Lin et al. (2011) applied model predictive control to control and coordinate urban traffic networks, for which the computation time is significantly reduced. Based on a model predictive control approach, Haddad et al. (2013) tackled the macroscopic traffic modeling and control of a large-scale mixed transportation network consisting of a freeway and an urban network, in order to minimize total delay for the entire network. By considering the uncertain passenger arrival flow, Li et al. (2016) applied model predictive control for train regulation in underground railways to ensure the minimization of an upper bound on the metro system cost function, showing that the proposed train regulation has a low online computation burden. This feature makes the MPC algorithm an ideal candidate for real-time metro traffic regulation.

1.3. Proposed approach and contributions

Note that there are many works on the study of train regulation methods for metro lines, which are mainly conducted by manipulating the running times and the dwell times of the trains. However, for peak hours with overloaded passengers, train regulation by just manipulating the running time and the dwell time of each train can not easily handle the overcrowded passenger flow. To the best of our knowledge, under the case that a disturbance or disruption occurs, few works pay attention to designing the train regulation by also considering the passenger flow control. Moreover, considering that existing nonlinear programming and dynamic programming methods become computationally prohibitive to deal with large optimization problems in real time, other approaches are needed to solve this problem. Based on the above consider-

Table 1
The comparison of different characteristics of related models and methods.

Characteristics	Research problem	Traffic model	Solution methodology	Stability property
Assis and Milani (2004)	Train schedule	Train and passenger load dynamics	Linear-programming-based Model predictive control	Did not verify system stability
Niu et al. (2015)	Train schedule	Train dynamics with passenger demand	Nonlinear mixed integer programming	Did not verify system stability
Van Breusegem et al. (1991)	Train regulation	Only train dynamics	Linear quadratic regulator	Verified system stability
Fernandez et al. (2006)	Train regulation	Only train dynamics	Quadratic programming	Did not verify system stability
Lin and Sheu (2010)	Train regulation	Only train dynamics	Dynamic programming	Did not verify system stability
Kang et al. (2015)	Train regulation	Only train dynamics	Genetic algorithm	Did not verify system stability
Yin et al. (2016)	Train regulation	Train dynamics with passenger demands	Approximate dynamic programming	Did not verify system stability
This paper	Train regulation and passenger flow control	Train and passenger load dynamics	Quadratic-programming-based Model predictive control	Verified system stability

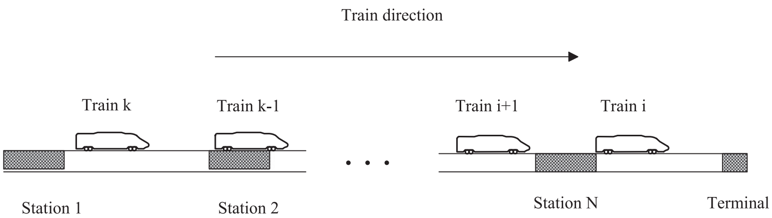

Fig. 1. The illustration of the metro-type railway line.

ations, this study focuses on the joint dynamic train regulation and passenger flow control design problem for metro lines to improve the headway regularity and commercial speed.

Specifically, the contributions of this paper are as follows.

(1) The dwell time of each train is affected by both the number of entering and exiting passengers. In contrast, existing studies usually do not consider passenger flow control in the train regulation problem (Yin et al., 2016; Li et al., 2016). By considering the sudden large passenger flow for high-frequency metro lines, this study constructs a coupled dynamic model for the evolution of both the train traffic and the passenger load, and designs a joint optimal train regulation and passenger flow control strategy. The proposed coupled dynamic model provides a new and more accurate insight for the train regulation problem.

(2) The proposed on-line optimization algorithm provides a real-time train regulation and passenger flow control strategy in the form of a closed loop system, which can be effectively and quickly implemented for practical metro lines in real-time. By using Lyapunov stability theory, the stability (convergence) characteristic of the metro line system has been verified under the proposed optimization algorithm.

The main features of our paper are summarized in Table 1 based on the four characteristics (research problem, traffic model, solution methodology and stability property) as compared to several related studies. The rest of this paper is organized as follows. In Section 2, a coupled dynamic model for the evolution of the departure time and the passenger load of each train is presented. In Section 3, the optimal joint train regulation and passenger flow control strategy for high-frequency metro lines is designed. In Section 4, numerical examples are provided to demonstrate the effectiveness of the proposed methods. We conclude this paper in Section 5.

2. Problem description

We consider a metro-type railway line with N stations and one terminal station, and an ordered set of trains are running on the stations and stop at the stations to allow passengers to embark and disembark. A metro-type railway line system mainly involves stations, trains and passengers. The aim of the operation management is to ensure the trains can transport all the passengers from their origin station to destination station in a safe and efficient way. An illustration for the operation of a metro-type railway line is shown in Fig. 1.

In real-time operations of metro lines, disturbances and disruptions are inevitable, such as equipment failure or inadequate driver/passenger actions, etc. When a disturbance or a disruption occurs, the optimized train timetable is not able to keep the original optimized objective, and a train regulation process has to be initiated to reduce train delays and the effect of the unpredicted events. Especially, during the peak hours of the day, the passenger demands for most of the stations are extremely large. As a result, when the train arrives at one station, the passenger load of the train is usually over its nominal passenger load. Under this case, if the passenger arrival flow is not controlled, the surplus passengers will try to get on the train, which will result in making the train delays even longer, and even worse the surplus passengers could lead to

Table 2
Indices and parameters used throughout the paper.

$i = 1, 2, \ldots, Z$:	indices of the trains on the line;
$j = 1, 2, \ldots, N$:	indices of the stations on the line;
System parameters	
R_j^i:	the nominal running time of train i from station j to station $j+1$;
D_j:	the minimal dwell time at a station when no passenger gets on the train;
α:	the delay rate for one passenger to get on or off a train;
β_j^i:	a disembarking proportionality factor at station j for train i;
γ_j^i:	the passenger arrival rate to station j for train i;
H:	the scheduled headway;
$l_{\max}$:	the maximum passenger load capacity of the train;
State variables	
t_j^i:	the actual departure time of the ith train from the jth station;
T_j^i:	the nominal departure time of the ith train from the jth station;
r_j^i:	the running time of the ith train from the jth station to the $j+1$th station;
s_j^i:	the dwell time of the ith train at the jth station;
l_j^i:	the actual load of train i between station j and $(j+1)$;
L_j^i:	the nominal load of train i between station j and $(j+1)$;
m_j^i:	the number of passengers entering train i at station j;
n_j^i:	the number of passengers exiting train i at station j;
${w_1}_j^i$:	the uncertain disturbance term to the running time;
${w_2}_{j+1}^i$:	the uncertain disturbance term to the dwell time;
T:	the considered time horizon;
M:	the finite prediction horizon;
Decision variables	
${u_1}_j^i$:	the control strategy to magnify the running time;
${u_2}_j^i$:	the dwell time adjustment;
p_j^i:	the control strategy to magnify the number of passengers.

a potential unsafe environment in the metro line system. Therefore, when trains deviate from their nominal time schedule under a disturbance or a disruption, it is necessary to consider both the train regulation strategy and the passenger flow control strategy to improve the safety and efficiency for the metro line system.

To address this problem, the train traffic dynamics are first constructed, and then the passenger load dynamics of the train are developed. Moreover, by combining the coupled relationship between the train traffic dynamics and the passenger load dynamics, the joint train traffic and passenger flow dynamic model is presented. Compared to the existing studies which used a time-dependent origin-destination (OD) matrix to represent passenger demands (Niu et al., 2015; Yin et al., 2016), this study applies a dynamic equation to describe the dynamic evolution of the passenger load of the train from one station to the next, which is determined by the number of entering and exiting passengers. The number of entering passengers is assumed to be proportional to the waiting time between successive trains (Fernandez et al., 2006; Lin and Sheu, 2010), which is time-dependent, and the number of the exiting passengers is assumed to be proportional to the number of passengers on the train (Eberlein et al., 2001), which is also time-dependent. Throughout this paper, the symbols and parameters are listed in Table 2.

2.1. The train traffic dynamics

Based on the discrete-event approach proposed by Van Breusegem et al. (1991), we present the train traffic dynamics according to the operation of high-frequency metro lines. The train traffic dynamics for the actual departure time of train i from station $j+1$ is given as follows.

$$t_{j+1}^i = t_j^i + r_j^i + s_{j+1}^i, \tag{1}$$

and the running time of train i from station j to $j+1$ is presented as

$$r_j^i = R_j^i + {u_1}_j^i + {w_1}_j^i, \tag{2}$$

where ${u_1}_j^i$ is the control strategy to magnify the running time of train i between stations j and $j+1$, which is applied to increase the running time when ${u_1}_j^i > 0$, and decrease the running time when ${u_1}_j^i < 0$. ${w_1}_j^i$ is the uncertain disturbance term to the running time (such as equipment failure or inadequate driver/passenger action).

Considering the fact that the dwell time of the train is affected by both the number of entering and exiting passengers, the dwell time s_{j+1}^i is modelled as

$$s_{j+1}^i = \alpha(m_{j+1}^i + n_{j+1}^i) + D_{j+1} + {u_2}_{j+1}^i + {w_2}_{j+1}^i, \tag{3}$$

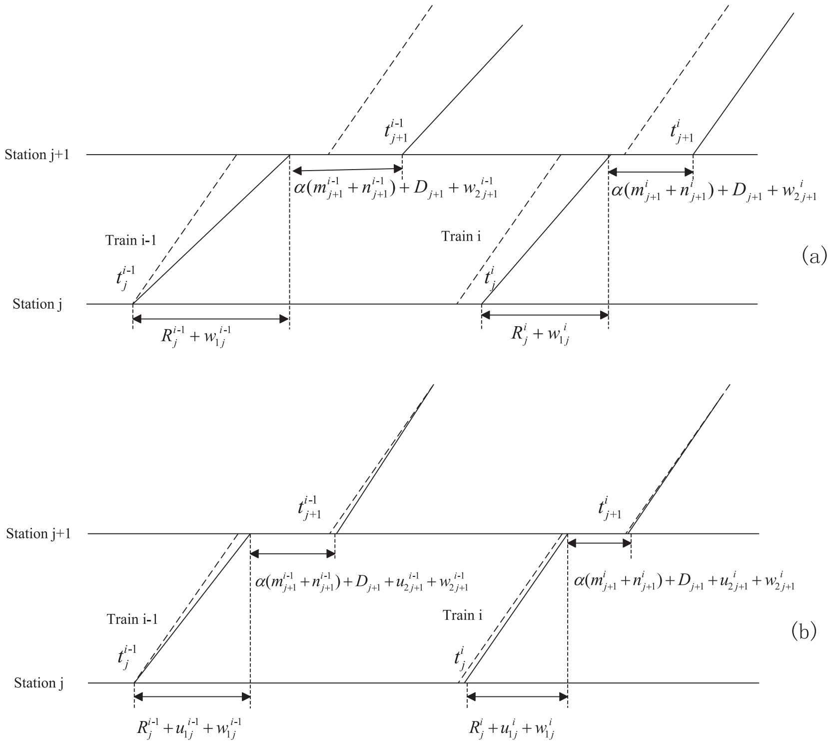

Fig. 2. An illustration of the train traffic dynamics.

where α is the delay rate representing the time necessary for one passenger to get on or off a train, m^i_{j+1} and n^i_{j+1} are the number of passengers entering and exiting train i at station $j+1$, respectively. ${u_2}^i_{j+1}$ is the dwell time adjustment on train i at station $j+1$, and ${w_2}^i_{j+1}$ is the uncertain disturbance term to the dwell time.

Then, by combining (1)–(3), the state-space model for the train traffic dynamics is described by

$$t^i_{j+1} = t^i_j + R^i_j + \alpha(m^i_{j+1} + n^i_{j+1}) + D_{j+1} + u^i_j + w^i_j, \tag{4}$$

where $u^i_j = {u_1}^i_j + {u_2}^i_{j+1}$ and $w^i_j = {w_1}^i_j + {w_2}^i_{j+1}$. An illustration of the train traffic dynamics for a metro line is plotted in Fig. 2, where Fig. 2(a) is the case without train regulation and Fig. 2(b) is the case with train regulation. The dotted line represents the nominal timetable, and the solid line denotes the actual train timetable.

From Fig. 2(a), we can find that when the disturbance occurs for the running time of train $i-1$ at station j, train $i-1$ is delayed when arriving at station $j+1$. At the same time, due to the delay of train $i-1$, the number of arriving passengers is increased, and the train delay increases at station $j+1$ with the accumulation of passengers. Furthermore, by the headway safety constraints, the next train i is also delayed from station j to station $j+1$. The train delay increases from one station to the next with the accumulation of passengers, which shows the instability of the metro line system. So it is necessary to implement train regulation to recover from the train delays and prevent the instability of the metro line operation. From Fig. 2(b), we can observe that under the train regulation strategy, by adjusting the running time and the dwell time of train $i-1$, and furthermore controlling the passenger arrival flow, the delay of train $i-1$ is effectively reduced, and the delay of train i is also reduced and recovered to the nominal timetable at station $j+1$.

2.2. The passenger load dynamics

When the train arrives at the station, there are passengers entering the train and passengers exiting the train. Then the dynamic evolution of the passenger load of the train at the station is given by

$$l^i_{j+1} = l^i_j + m^i_{j+1} - n^i_{j+1} + p^i_{j+1}. \tag{5}$$

where p^i_{j+1} is the control strategy to magnify the number of passengers entering train i at station $j+1$, which is implemented during rush hour or on a special holiday for the sudden gathering of passengers, and thus is a non-positive value to reduce the passenger load. Under the control strategy for the passenger flow, the actual number of passengers entering the train is changed to $m^i_{j+1} + p^i_{j+1}$. In addition, the passenger load dynamic is mainly determined by the number of entering and exiting passengers and not affected by the external disturbance.

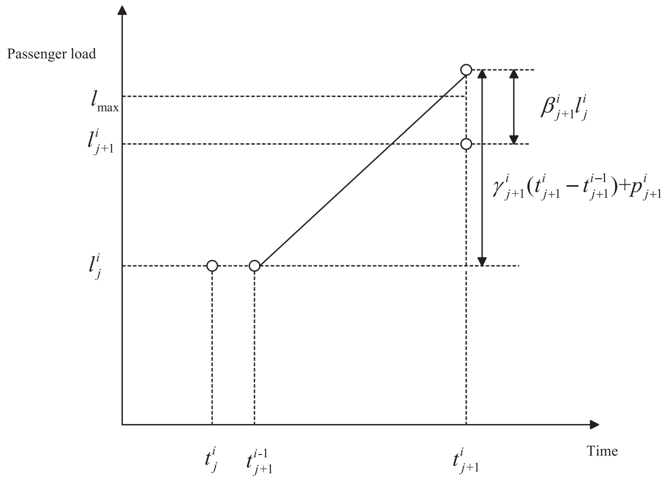

Fig. 3. The illustration of the passenger load dynamics of the train.

The number of entering passengers m^i_{j+1} is assumed to be proportional to the waiting time between successive trains, which is given as

$$m^i_{j+1} = \gamma^i_{j+1}(t^i_{j+1} - t^{i-1}_{j+1}), \tag{6}$$

where γ^i_{j+1} represents the passengers arrival rate, which can be measured in real time by the monitoring techniques (Fernandez et al., 2006). Here it should be pointed out that if the number of entering passengers is large and results in an overload of the train, the control strategy p^i_{j+1} is conducted to reduce the number of entering passengers to satisfy the limited capacity of the train for carrying passengers. In particular, with the control strategy for the passenger flow, the actual dwell time s^i_{j+1} is changed to

$$s^i_{j+1} = \alpha(m^i_{j+1} + n^i_{j+1} + p^i_{j+1}) + D_{j+1} + {u_2}^i_{j+1} + {w_2}^i_{j+1}, \tag{7}$$

which shows the control strategy for the passenger flow not only adjusting the number of passengers entering the train, but also changing the dwell time of the train. Moreover, we assume that the train stops at each station. The state constraint for the passenger load is considered to satisfy the requirement of the maximum capacity of the train, and the control constraint for the running time adjustment u_{1ij} and dwell time adjustment u_{2ij} is considered to ensure that the final dwell time is larger than the minimum required dwell time D_j and meanwhile the speed constraint is satisfied for the running time adjustment.

The number of exiting passengers is assumed to be proportional to the number of passengers in the train. That is, the number of exiting passengers is equal to

$$n^i_{j+1} = \beta^i_{j+1} l^i_j \tag{8}$$

where l^i_j is the load of train i between station j and $j+1$, and β^i_{j+1} is a proportionality factor that depends on station $j+1$ and on the hour of travel for train i, which is statistically estimated from the passenger demand OD matrices during the specific time periods of the day, and thereby represents the OD demand from different OD pairs for each station. In addition, different to the time-dependent OD matrix adopted in Niu et al. (2015) and Yin et al. (2016), the dynamic Eq. (5) describes the dynamic evolution of the passenger load from one station to the next one for each train, which facilitates to design the dynamic passenger flow control to adjust the overload of the train.

Then by combining (5)–(8), the passenger load dynamics of the train can be written as

$$l^i_{j+1} = l^i_j + \gamma^i_{j+1}(t^i_{j+1} - t^{i-1}_{j+1}) - \beta^i_{j+1} l^i_j + p^i_{j+1}, \tag{9}$$

which indicates that the passenger load dynamics of the train is also affected by the train traffic dynamics. Moreover, the illustration for changing the load of the train for carrying passengers is plotted in Fig. 3, in which the passenger load dynamics is affected by the departure time of the train.

2.3. The joint dynamic model

By combining the above Eqs. (4) and (9), we can obtain the joint dynamic model of the departure time and the passenger load of the train as follows.

$$\begin{cases} t^i_{j+1} = t^i_j + R^i_j + \alpha(\gamma^i_{j+1}(t^i_{j+1} - t^{i-1}_{j+1}) + \beta^i_{j+1} l^i_j + p^i_{j+1}) + D_{j+1} + u^i_j + w^i_j, \\ l^i_{j+1} = l^i_j + \gamma^i_{j+1}(t^i_{j+1} - t^{i-1}_{j+1}) - \beta^i_{j+1} l^i_j + p^i_{j+1}, \end{cases} \tag{10}$$

which shows that the departure time and the passenger load of the train influence each other. From Eq. (10), we can also observe that if one train is delayed, the train delay increases from one station to the next station with the accumulation of passengers, which indicates the possible instability of the metro line.

Let $x_j^i = [t_j^i, l_j^i]^T$ and $\bar{u}_j^i = [u_j^i, p_{j+1}^i]^T$. According to Eq. (10), the joint dynamic model of the departure time and the passenger load of the train can be obtained together as.

$$x_{j+1}^i = A_j^i x_j^i + B_j^i x_{j+1}^{i-1} + C_j^i \bar{u}_j^i + G_j^i (D_{j+1} + R_j^i + w_j^i). \tag{11}$$

where $x_j^0 = [0,0]^T$, $A_j^i = \begin{bmatrix} \frac{1}{1-\alpha\gamma_{j+1}^i} & \frac{\alpha\beta_{j+1}^i}{1-\alpha\gamma_{j+1}^i} \\ \frac{\gamma_{j+1}^i}{1-\alpha\gamma_{j+1}^i} & 1-\beta_{j+1}^i + \frac{\alpha\gamma_{j+1}^i\beta_{j+1}^i}{1-\alpha\gamma_{j+1}^i} \end{bmatrix}$, $B_j^i = \begin{bmatrix} \frac{-\alpha\gamma_{j+1}^i}{1-\alpha\gamma_{j+1}^i} & 0 \\ \frac{-\gamma_{j+1}^i}{1-\alpha\gamma_{j+1}^i} & 0 \end{bmatrix}$, $C_j^i = \begin{bmatrix} \frac{1}{1-\alpha\gamma_{j+1}^i} & \frac{\alpha}{1-\alpha\gamma_{j+1}^i} \\ \frac{\gamma_{j+1}^i}{1-\alpha\gamma_{j+1}^i} & \frac{1}{1-\alpha\gamma_{j+1}^i} \end{bmatrix}$, $G_j^i = \begin{bmatrix} \frac{1}{1-\alpha\gamma_{j+1}^i} \\ \frac{\gamma_{j+1}^i}{1-\alpha\gamma_{j+1}^i} \end{bmatrix}$. The derivation of (11) is given in Appendix A.

The joint dynamic model describes the dynamic changing of the departure time and the passenger load of the train, which provides a more general model for the operation management of the metro line system under disturbance or disruption.

It is a common practice to operate with different scheduled headway for different operating hours, e.g., peak and off-peak hours. Then for a specific duration of operating hours, a nominal joint traffic and passenger flow model can be constructed as follows.

$$T_{j+1}^i = T_j^i + R_j^i + \alpha(\gamma_{j+1}^i (T_{j+1}^i - T_{j+1}^{i-1}) + \beta_{j+1}^i L_j^i) + D_{j+1} \tag{12}$$

and

$$L_{j+1}^i = L_j^i + \gamma_{j+1}^i (T_{j+1}^i - T_{j+1}^{i-1}) - \beta_{j+1}^i L_j^i. \tag{13}$$

The nominal timetable is characterized by a constant time interval H between two successive trains, i.e., $H = T_{j+1}^i - T_{j+1}^{i-1}$. The scheduled headway H of the corresponding operating hours is determined by the service operating requirement, capacity of the train and passenger flow of the operating hours. In particular, the scheduled headway H is smaller during the peak hours.

Moreover, to improve the headway regularity and commercial speed, we define the error vector as $e_j^i = [t_j^i - T_j^i, l_j^i - L_j^i]^T$. According to (12) and (13), together with (11), we can obtain the error dynamics for the joint dynamic model as follows.

$$e_{j+1}^i = A_j^i e_j^i + B_j^i e_{j+1}^{i-1} + C_j^i \bar{u}_j^i + G_j^i w_j^i. \tag{14}$$

where A_j^i, B_j^i, C_j^i, and G_j^i take the same forms as in (11). The derivation of (14) is given in Appendix B.

Remark 2.1. For the error dynamics (14), noting that e_j^i represents the deviations of the actual departure time of the train from the nominal departure time and the actual passenger load of the train from the nominal passenger load, then the minimization of $\|e_j^i\|$ means to improve the operational efficiency of the metro line for recovering train delays from disturbances. Moreover, if $e_j^i \to 0$, then $t_j^i \to T_j^i$ and $l_j^i \to L_j^i$, which prevents the instability of the metro line operation. Therefore, the stability of the metro line operation is converted to the stability problem of the dynamic system (14) at zero, which facilitates applying system stability theory to derive the stability condition of metro line operations. To conveniently apply system stability theory, we further define the matrix form of the joint dynamic model in the next section.

2.4. The matrix form of the joint dynamic model

For the train traffic model of metro lines, there are mainly three types of models (Van Breusegem et al., 1991), which are station sequential model (SSM), train sequential model (TSM), and real time model (RTM). In these three models, the station sequential model (SSM) is always applied for the generation of the train timetables (Cury et al., 1980; Assis and Milani, 2004), while the real time model (RTM) is the only one that allows for a complete on-line feedback control (Van Breusegem et al., 1991). In this paper, we adopt the real time model (RTM) to describe the train operations of metro lines. According to (11), we now propose the formulation for the joint dynamic model based on information propagation considerations, that is, x_{j+1}^i is generated by x_j^i and x_{j+1}^{i-1} for all the trains and stations. Then, regarding the variable X_k, the state variable of the matrix form for the joint dynamic model is considered as $X_k = [x_1^{k-1}, x_2^{k-2}, \ldots, x_N^{k-N}]^T$, which denotes the departure time of the trains and the passenger load of the trains at all the stations, where the index $k > N$. The dimension of the state variable X_k is double the number of stations for the metro line. Here we assume that the components of the state vector X_k are all located at the same time interval. Because of the traffic security requirements for metro lines (e.g. at most one train at a time in a section between two successive stations), the deviations x_j^i (train i at station j) and x_{j+1}^{i-1} (preceding train at the next station) are known in a short time, i.e, all the components of X_k are known in a short time

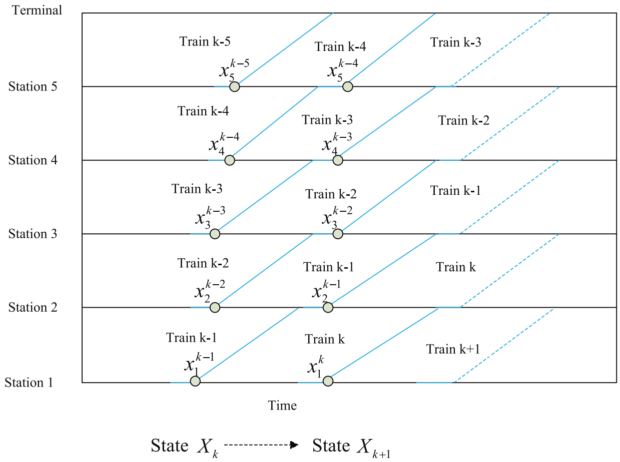

Fig. 4. The illustration of the transfer from state X_k to state X_{k+1}.

(Van Breusegem et al., 1991). Thus, this assumption is rational. To show the state variable X_k clearly, we take an example for a metro line with $N = 5$ stations, and the illustration of the transfer from state X_k to state X_{k+1} is plotted in Fig. 4, in which $X_k = [x_1^{k-1}, x_2^{k-2}, x_3^{k-3}, x_4^{k-4}, x_5^{k-5}]^T$ and $X_{k+1} = [x_1^{k}, x_2^{k-1}, x_3^{k-2}, x_4^{k-3}, x_5^{k-4}]^T$. In particular, it should be noted that for stage k, x_1^{k-1} represents the state of the $(k-1)$th train at station 1. Similarly, x_2^{k-2} is the state of the $(k-2)$th train at station 2.

Then by combining (11), the matrix form of the joint dynamic model can be expressed as

$$X_{k+1} = \bar{A}_k X_k + \bar{B}_k U_k + \bar{G}_k (w_k + R_k + D), \tag{15}$$

where k indexes the stage of the joint dynamic model, X_k is the state vector (consisting of the departure time and the passenger load of the train), the control vector $U_k = [\bar{u}_0^k, \bar{u}_1^{k-1}, \dots, \bar{u}_{N-1}^{k-N+1}]^T$, the disturbance vector $w_k = [w_0^k, w_1^{k-1}, \dots, w_{N-1}^{k-N+1}]^T$, and its dimension is N, $R_k = [R_0^k, R_1^{k-1}, \dots, R_{N-1}^{k-N+1}]^T$, $D = [D_1, D_2, \dots, D_N]^T$, and the definitions of matrices $\bar{A}_k$, $\bar{B}_k$, and $\bar{G}_k$ are given in Appendix C.

According to the matrix form of the joint dynamic model (15), the system dimension is $2N$, which is only related to the number of stations in the metro line and not related to the number of trains. Moreover, the system matrix $\bar{A}_k$ describes the intrinsically coupled dynamic relationship between the train traffic dynamics and the train load dynamics, the control matrix $\bar{B}_k$ represents the coupled relationship between the train regulation and passenger flow control, and the matrix $\bar{G}_k$ is related to the system parameters for the disturbance.

Moreover, according to (14), the matrix form of the joint error dynamic model is obtained as

$$E_{k+1} = \bar{A}_k E_k + \bar{B}_k U_k + \bar{G}_k w_k, \tag{16}$$

where the error state vector $E_k = [e_1^{k-1}, e_2^{k-2}, \dots, e_N^{k-N}]^T$, which consists of errors of the departure time and the passenger load deviations away from the nominal state. And the meaning of the system parameters $\bar{A}_k$, $\bar{B}_k$, and $\bar{G}_k$ are the same to that as in formula (15).

It should be noted that the proposed joint error dynamic model (16) is in fact a linear time-varying discrete systems, in which the system parameters $\bar{A}_k$, $\bar{B}_k$, and $\bar{G}_k$ and the disturbance w_k are changing with time, and not pre-known. The traditional dynamic programming method is hard to deal with this system (16) with real-time updated system parameters. It requires an on-line optimization technique to deal with this system (16). A model predictive control (MPC) algorithm, as an on-line optimization technique, can be implemented to cope with system (16) with real-time updating system parameters and disturbance.

3. Problem formulation and solution

3.1. Problem formulation

The design of the joint dynamic train regulation and passenger flow control strategy for metro lines is to improve the headway regularity and commercial speed. To address this problem, we consider the following cost function for the joint dynamic model of metro lines.

$$J = \sum_{i,j} \left\{ {e_j^i}^T P_j^i e_j^i + (e_j^i - e_j^{i-1})^T Q_j^i (e_j^i - e_j^{i-1}) + (\bar{u}_j^i)^T R_j^i \bar{u}_j^i \right\}, \tag{17}$$

where P_j^i, Q_j^i, and R_j^i are given positive definite weighted matrices. The first term in (17) denotes the sum of the errors of the actual timetable from the nominal timetable and the actual load of the train from the nominal load, which is used for reducing the deviation of the practical timetable and the load of the train to improve the commercial speed. The weighted matrix $P_j^i = \begin{bmatrix} b_{1j}^{\,i} & 0 \\ 0 & b_{2j}^{\,i} \end{bmatrix}$, where $b_{1j}^{\,i}$ is the weight for the timetable error $t_j^i - T_j^i$ and $b_{2j}^{\,i}$ is the weight for the train load error $l_j^i - L_j^i$. During the peak hours with the overcrowded passenger arrival flow, the actual train load is usually larger than the nominal load. Under this case, the minimization of $b_{2j}^{\,i}(l_j^i - L_j^i)^2$ means that the passenger control should be implemented to reduce the train load l_j^i. Otherwise, for the case that the actual train load without passenger flow control is less than the nominal load, we can get that $l_{j-1}^i + m_j^i - n_j^i < L_j^i$ according to the dynamic Eq. (5). Under this case, if we further consider the passenger flow control, the minimization of the quadratic function $b_{2j}^{\,i}(l_j^i - L_j^i)^2$ for the actual train load l_j^i with the control variable p_j^i is equivalent to the minimization of $b_{2j}^{\,i}(l_{j-1}^i + m_j^i - n_j^i + p_j^i - L_j^i)^2$, where the only decision variable is p_j^i. Consider that the control variable p_j^i is non-positive ($p_j^i \le 0$) and $l_{j-1}^i + m_j^i - n_j^i < L_j^i$. Then, it is clear that the minimization of $b_{2j}^{\,i}(l_{j-1}^i + m_j^i - n_j^i + p_j^i - L_j^i)^2$ implies that the control variable $p_j^i = 0$, i.e., the control action p_j^i is not required, which satisfies the practical requirement. In the literature, this type of the quadratic performance index for the train load errors has be also adopted by Campion et al. (1985). Therefore, it is reasonable to adopt quadratic functions to minimize the train load errors under the proposed passenger flow control framework. For the second term of (17), we choose the weighted matrix Q_j^i of the form $Q_j^i = \begin{bmatrix} q_j^i & 0 \\ 0 & 0 \end{bmatrix}$, where $q_j^i > 0$ is a given constant. Then the second term is related to headway deviation of the trains, which is used for improving the headway regularity, and meanwhile reducing the average waiting time for the passengers. The third term deals with the amplitude of the control action. The minimization of the amplitude of the control action is used to penalize the control actions that are too large, so as to reduce the control cost in practical applications (Van Breusegem et al., 1991; Fernandez et al., 2006).

In metro-type railways operated according to an offered timetable, deviations are usually measured by two performance indicators, namely, punctuality and regularity, where punctuality refers to the deviations of the actual departure time from the nominal departure time (timetable errors), whereas regularity refers to the headway deviations between consecutive departures (Mannino and Mascis, 2009). When the disturbances happen, the reduction of the headway deviations does not ensure that the deviations of the actual departure time can be reduced, which may increase the deviations of the actual departure time. Thus, the train regulation seeks a compromise between timetable (the actual departure time) and headway deviations during the transient period (Van Breusegem et al., 1991; Fernandez et al., 2006; Lin and Sheu, 2010). The weighted matrices P_j^i and Q_j^i in (17) depend on the practical control purpose and reflect the trade-off between the regulation objectives (the headway regularity and commercial speed).

Moreover, based on the definition of the matrix form for the joint dynamic model (16), the matrix form of the objective function (17) is formulated as follows.

$$J = \sum_{k=j_0}^{j_f} \left\{ E_k^T P E_k + (E_{k+1} - E_k)^T Q (E_{k+1} - E_k) + U_k^T R U_k \right\}, \tag{18}$$

where P, Q and R are given positive definite weighted matrices, which are composed of P_j^i, Q_j^i, and R_j^i and can be directly obtained from (17). j_0 and j_f are the initial and terminal state numbers, respectively.

In addition, to ensure the safe operation of the metro line, we consider the following constraints.

(1) State constraints for the departure time: To ensure the safety distance between two neighbouring trains, we have $t_j^i - t_j^{i-1} \ge t_{\min}$, where $t_{\min}$ is the minimum allowable safety headway. Moreover, the state constraints for the departure time of each train can be converted as the error state constraints for the departure time of each train, which is given as

$$(t_j^i - T_j^i) - (t_j^{i-1} - T_j^{i-1}) \ge t_{\min} - H, \tag{19}$$

where $t_{\min}$ and H are given.

(2) State constraints for the passenger load: To satisfy the requirement of the capacity of the train, the load of the train l_j^i has the constraint: $l_j^i \le l_{\max}$, where $l_{\max}$ is the maximum capacity of the train for passengers. Similarly, it can be converted as the error state constraints for the passenger load of the train, which is presented as

$$(l_j^i - L_j^i) \le l_{\max} - L_j^i, \tag{20}$$

where $l_{\max}$ and L_j^i are given.

(3) Control constraints: For the practical limits for the control input, we consider the following control constraints

$$[u_{\min}, p_{\min}]^T \le \bar{u}_j^i \le [u_{\max}, p_{\max}]^T \tag{21}$$

where $[u_{\min}, p_{\min}]$ is the minimum allowable vector for the control input and $[u_{\max}, p_{\max}]$ is the maximum allowable vector for the control input, and here $p_{\max} = 0$ according to Eq. (5).

Then, according to the matrix form of the joint dynamic model, the above constraints can be rewritten in the following matrix form.

(1) State constraints for the departure time:

$$H_1(E_{k-1} - E_k) \leq (H - t_{\min})I_{N\times 1}, \tag{22}$$

where H_1 is a matrix of dimension $N \times 2N$, in which for each row i of the matrix, the element $H_1(i, 2i-1) = 1$, and all other elements for this row equal to zero, $I_{N \times 1}$ is a matrix with $N \times 1$ dimension, and all the elements equal to 1.

(2) State constraints for the passenger load:

$$H_2 E_k \leq L_k, \tag{23}$$

where H_2 is a matrix of dimension $N \times 2N$, in which for each row i of the matrix, the element $H_2(i, 2i) = 1$, and all other elements for this row equal to zero, $L_k = [l_{\max} - L_1^{k-1}, l_{\max} - L_2^{k-2}, \ldots, l_{\max} - L_N^{k-N}]^T$.

(3) Control constraints:

$$U_k \leq U_{\max}, -U_k \leq -U_{\min}, \tag{24}$$

where $U_{\max}$ is a column vector of dimension $2N$ for which the elements in the odd rows equal $u_{\max}$, and in the even rows equal $p_{\max}$. Similarly, $U_{\min}$ is also a column vector of $2N$ dimension for which the elements in the odd rows equal $u_{\min}$, and in the even rows equal $p_{\min}$.

Given the train traffic dynamics and the passenger load dynamics of the previous section, by considering the matrix form of the joint dynamic model (16) and the objective function (18), the joint train regulation and passenger flow control problem can be converted to the problem of solving the following optimal control problem:

$$\min_{U_k} \sum_{k=j_0}^{j_f} \left\{ E_k^T P E_k + (E_k - E_{k-1})^T Q (E_k - E_{k-1}) + U_k^T R U_k \right\} \tag{25}$$

$$\begin{aligned}
\text{s.t. } & E_{k+1} = \bar{A}_k E_k + \bar{B}_k U_k + \bar{G}_k w_k, \\
& H_1(E_{k-1} - E_k) \leq (H - t_{\min})I_{N\times 1}, \\
& H_2 E_k \leq L_k, \\
& U_k \leq U_{\max}, \\
& -U_k \leq -U_{\min}.
\end{aligned}$$

For the above optimal control problem (25), the first constraint is the state equation, the second and third are state constraints and the last two constraints are the control constraints. Since the system parameters $\bar{A}_k$, $\bar{B}_k$, and $\bar{G}_k$ and the disturbance w_k are time-dependent, a traditional dynamic programming method with pre-known system parameters is hard to deal for the above optimal control problem. To handle it, we adopt a model predictive control algorithm, an on-line optimization technique, to solve the formulated optimal control problem (25).

3.2. The MPC algorithm

Model predictive control (MPC) is a control methodology that implements repeatedly optimal control in a rolling horizon manner. In MPC, at each sample step k, we compute an optimal control input that minimizes a given cost function over a pre-specified prediction horizon. The illustration for the principle of the MPC for the optimal control problem (25) is plotted in Fig. 5, where the circled lines represent the measured and predicted states, and the solid lines denote the optimal control sequence.

As shown in Fig. 5(a), at each sample step k, the optimal control problem is solved online based on the measured current state E_k (the errors of the departure time of the trains from the nominal state and the errors of the passenger loads from the nominal state at stage k) over an M step finite prediction horizon $(k+1, \ldots, k+M)$, and a set of optimal control sequence are obtained as $U_k, U_{k+1}, \ldots, U_{k+M-1}$. The prediction states E_{k+i} are calculated based on the evolution of the state of the system (16) under control. In order to take into account the changes of the system parameters and disturbances, at each sample step k, only the first control vector U_k (joint train regulation and passenger flow control at stage k) of the optimal control sequence is implemented to the system, which can be observed in Fig. 5(b). At the next step $k+1$, the optimal control problem is solved again with the newly updated information of the measurement state E_{k+1}, and also only the first control vector is applied to the system, and so forth. Within the framework of MPC, a set of optimization problems are repeatedly solved online in a rolling horizon manner based on the real-time updated system information, which makes this method efficient to solve the above optimal control problem (25) with the updated system parameters and disturbances.

Specifically, the MPC approach for the metro lines can be characterized by the following three components:

(1) The prediction model of system.

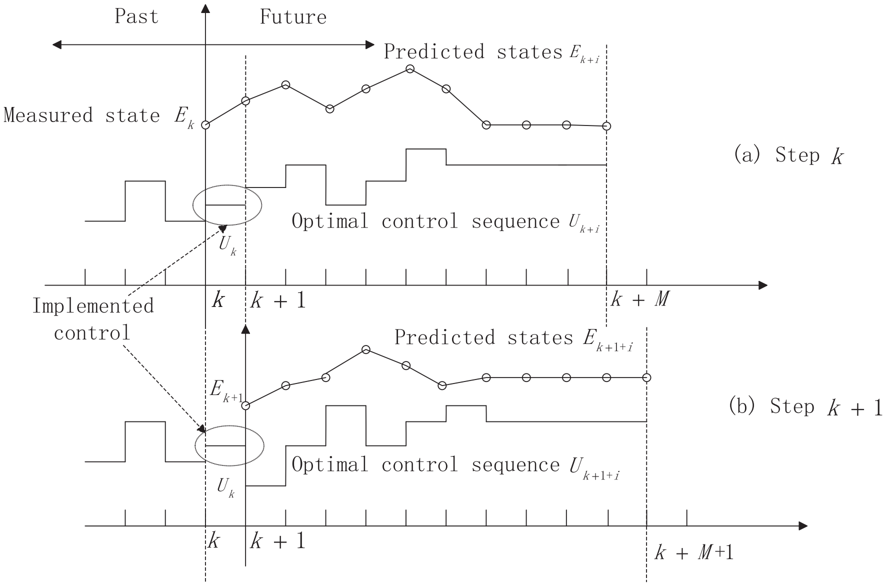

Fig. 5. An illustration of the principle of the MPC.

The prediction model of the dynamic system is used to predict the effects of the control inputs on the evolution of the dynamic system over a given prediction horizon and to determine the control strategy that optimizes a given cost function. For the metro line system, the proposed model (16) of the metro line system is used to predict the future errors of the departure time of the trains and the future errors of the passenger loads of the trains based on the measured current state E_k.

(2) The optimization problem.
Based on the model of the dynamic system, at each sample step k, the optimization problem over a given prediction horizon is solved online, which determines a set of optimal control sequences. For the metro line system, the optimization determines the joint train regulation and passenger flow control strategy that improves the headway regularity and commercial speed of high-frequency metro lines under the constraints based on the updated information of the measurements. Specially, at each sample step k, associated with (25) is the following optimization problem to compute the control input.

$$\min_{U_{k+j}} \sum_{j=0}^{M-1} \left\{E_{k+j+1}^T P E_{k+j+1} + (E_{k+j+1} - E_{k+j})^T Q (E_{k+j+1} - E_{k+j}) + U_{k+j}^T R U_{k+j}\right\} \tag{26}$$

$$\begin{aligned} \text{s.t. } & E_{k+j+1} = \bar{A}_{k+j} E_{k+j} + \bar{B}_{k+j} U_{k+j} + \bar{G}_{k+j} w_{k+j}, \\ & H_1 (E_{k+j} - E_{k+j+1}) \le (H - t_{\min}) I_{N\times 1}, \\ & H_2 E_{k+j+1} \le L_{k+j+1}, \\ & U_{k+j} \le U_{\max}, \\ & -U_{k+j} \le -U_{\min}, \quad j = 0, 1, \ldots, M-1. \end{aligned}$$

(3) The rolling horizon.
When the optimal control input is obtained from the optimization, the first control vector of the optimal result is implemented to the process. At the next step $k+1$, the prediction model (16) of the metro line system receives the new measured information, the whole prediction horizon is shifted one step forward, and the optimization starts again. This rolling horizon scheme makes MPC a closed-loop control, which enables the system to get feedback from real time information.

Moreover, at each sample step k, the above optimization problem (26) can be converted to a quadratic programming (QP) problem. Define $E = [E_{k+1}^T, E_{k+2}^T, \ldots, E_{k+M}^T]^T$ and $U = [U_k^T, U_{k+1}^T, \ldots, U_{k+M-1}^T]^T$. Then at each prediction step k, for the measured current state E_k, the state prediction for the M step finite horizon problem is obtained from the state equation of (26) as follows.

$$E = F E_k + \Phi U, \tag{27}$$

where the definitions of matrices F and Φ are given in Appendix C.

Thus the optimal joint train regulation and passenger flow control strategy is reduced to the problem of solving a set of quadratic programming (QP) problems at different steps. According to Eq. (26), the equivalent QP formulation at step k for the optimization problem (26) is presented as follows.

$$\min_{U} \; J = U^T(\Phi^T\bar{P}\Phi + \Phi^T\bar{Q}\Phi + \bar{R})U + 2U^T(\Phi^T\bar{P}FE_k + \Phi^T\bar{Q}FE_k) + \Psi \tag{28}$$

$$\text{s.t.} \begin{bmatrix} H_3H_4\Phi \\ H_6\Phi \\ I_{2MN} \\ -I_{2MN} \end{bmatrix} U \le \begin{bmatrix} (H - t_{\min})I_{MN\times 1} - H_3H_4FE_k - H_3H_5E_k \\ L - H_6FE_k \\ \bar{U}_{\max} \\ -\bar{U}_{\min} \end{bmatrix},$$

where $\Psi = F^T\bar{P}FE_k^2 + F^T\bar{Q}FE_k^2$ is a constant, the weighted matrixes $\bar{P}$, $\bar{Q}$ and $\bar{R}$ can be directly obtained from the cost function of (26), $L = [L_{k+1}^T, L_{k+2}^T, \ldots, L_{k+M}^T]^T$, $\bar{U}_{\max} = [U_{\max}^T, U_{\max}^T, \ldots, U_{\max}^T]^T_{2MN\times 1}$, $\bar{U}_{\min} = [U_{\min}^T, U_{\min}^T, \ldots, U_{\min}^T]^T_{2MN\times 1}$. The derivation of (28) from (26) is given in Appendix D. The other matrices H_3, H_4, H_5, H_6 are defined in Appendix D.

According to the formulated quadratic programming (QP) problem, the main algorithm of the joint optimal train regulation and passenger flow control strategy for metro lines under disturbances is summarized as follows.

Algorithm 3.1.

- *Step 1. At each sample step k, obtain the measured state E_k for the error joint dynamic model (16) with the undated parameters and disturbances.*
- *Step 2. According to the measured state* E_k*, for the given prediction horizon* M*, calculate the system parameters* F *and* Φ *for the error joint dynamic model (16)based on the formulation (27).*
- *Step 3. For the measured state E_k and obtained system parameters F and Φ, formulate the quadratic programming (QP) problem (28).*
- *Step 4. By solving the quadratic programming(QP) problem (28), get the joint optimal train regulation and passenger flow control strategy U and apply it to the joint dynamic model (16) to obtain the next value E_{k+1}.*
- *Step 5. Based on the measured value E_{k+1}, repeat Steps 1–4 until the step horizon j_f.*

It should be noted that the measured current state E_k includes the current errors of the departure time of train from the nominal state $(t_j^i - T_j^i)$ and the current errors of the passenger loads from the nominal state $(l_j^i - L_j^i)$. At each decision step, the actual departure time of trains can be easily obtained by the metro regulation department. In particular, with the highly developed monitoring equipments applied in each carriage of the train, the actual passenger load of trains at each decision step can be measured more accurately. The actual passenger loads of each train are also available during the algorithm execution. Thus, the system states (departure time and passenger load) of metro lines are fully observable. In addition, at each step k, based on the measured current state E_k, we need to predict the near-future states (departure time and passenger load) of trains over an M step finite prediction horizon $(k+1, \ldots, k+M)$ during a short time period, where the states of the trains at stage $k+M$ is the “boundary” which is not controlled. Within the framework of MPC, we use a dynamic evolution model (16) to predict the near-future states of the trains based on the measured current state E_k. For the system parameters of (16), we assume that the passenger arrival rate γ_j^i does not change during a short time period of the prediction horizon, which is chosen from the measured value at step k. The disembarking proportionality factor β_j^i during the prediction horizon is chosen from the estimated values by using the historical data.

According to the proposed MPC algorithm, the optimal control problem (25) for the joint optimal train regulation and passenger flow control strategy is formulated as a set of quadratic programming(QP) problems. By choosing the proper prediction step, the proposed MPC algorithm can reduce the number of variables and constraints for the formulated quadratic programming(QP) problems, which leads to a low online computational burden of the MPC algorithm. Thus the proposed MPC algorithm is effective in dealing with the large-scale nonlinear optimization problem for metro lines.

3.3. Stability analysis

In practice, due to the instability of many metro line systems, it is desirable to design a train regulation algorithm to ensure stability of the metro line. To further reveal the feature of the proposed MPC algorithm for the joint optimal train regulation and passenger flow control strategy, we analyze the stability (convergence) of the metro line system under the proposed MPC algorithm.

The stability of the metro line system under the MPC algorithm is a complex function of the MPC parameters P, Q, R, $\bar{A}_k$, $\bar{B}_k$, L_k, $U_{\max}$ and $U_{\min}$. Consider the state and control constraints for the metro line system with the overcrowded passenger arrival flow. It becomes more difficult to analyze the system stability. In particular, MPC has the advantage to cope with hard constraints on states and controls of the system. MPC of constrained systems is nonlinear necessitating the use of Lyapunov stability theory for system stability analysis. The value function of the optimization problem could be employed as a Lyapunov function for establishing stability of the model predictive control of the constrained discrete-time system (Mayne et al., 2000). Correspondingly, for the proposed MPC algorithm in this study, one can also apply the value function of the optimization problem (25) as a Lyapunov function to analyze the stability of the metro line system with state and control constraints.

To discuss the stability of the metro line system, we consider the joint error dynamic model (16) without disturbances w_j, i.e., $w_j = 0$. Then based on Lyapunov stability theory, we present the stability result of the joint error dynamic model under the proposed MPC algorithm as the following theorem.

Theorem 3.1. *Consider the joint error dynamic model (16) under the proposed MPC algorithm based on the following optimization problem*

$$\min_U J(U, E_k) = \sum_{j=0}^{M-1} \left\{ E_{k+j+1}^T P E_{k+j+1} + (E_{k+j+1} - E_{k+j})^T Q (E_{k+j+1} - E_{k+j}) + U_{k+j}^T R U_{k+j} \right\} \tag{29}$$

$$\begin{aligned} \text{s.t. } & E_{k+j+1} = \bar{A}_{k+j} E_{k+j} + \bar{B}_{k+j} U_{k+j} + \bar{G}_{k+j} w_{k+j}, \\ & H_1 (E_{k+j} - E_{k+j+1}) \le (H - t_{\min}) I_{N\times 1}, \\ & H_2 E_{k+j+1} \le L_{k+j+1}, \\ & U_{k+j} \le U_{\max}, \\ & -U_{k+j} \le -U_{\min}, \quad j = 0, 1, \ldots, M-1. \end{aligned}$$

Suppose that the above optimization problem is feasible at the initial time $k = j_0$, the system parameters $\bar{A}_k$ and $\bar{B}_k$ are given, and $E_{k+M} = 0$. Then for all $P > 0$, $Q > 0$, and $R > 0$, it holds that $\lim_{k\to\infty} E_k = 0$, that is, the joint error dynamic model (16) under the proposed MPC algorithm is stable at zero subject to the constraints, and the actual timetable converges to the nominal timetable.

Proof. At first, for the joint error dynamic model (16) under the proposed MPC algorithm, we choose the value function of the above optimization problem (29) as a Lyapunov function, i.e.,

$$V(k) = J(U^*(k), E_k), \tag{30}$$

where $U^*(k) = \{U_k^*, U_{k+1}^*, \ldots, U_{k+M-1}^*\}$ denotes the optimal control sequence for the optimal problem (29). It is clear that $V(k)$ is non-negative.

Then for the optimal control solutions $U^*(k)$ at step k, we can further get the state vector $E(k) = [E_{k+1}^T, E_{k+2}^T, \ldots, E_{k+M}^T]^T$ at step k. It is clear that $U^*(k)$ and $E(k)$ satisfy the constraints. Thus for the next step $k+1$, we construct the control sequence $U(k+1) = \{U_{k+1}^*, U_{k+2}^*, \ldots, U_{k+M-1}^*, 0\}$. It is clear that $U(k+1)$ is feasible at step $k+1$ for the optimal problem (29). By substituting $U(k+1)$ into the objective function, we can obtain $J(U(k+1), E_{k+1})$. Then by combining the assumption $E_{k+M} = 0$, we have

$$\begin{aligned} V(k+1) &= J(U^*(k+1), E_{k+1}) \\ &\le J(U(k+1), E_{k+1}) \\ &= V(k) - E_{k+1}^T P E_{k+1} - (E_{k+1} - E_k)^T Q (E_{k+1} - E_k) - U_k^T R U_k, \end{aligned} \tag{31}$$

which means that $V(k+1) - V(k) \le 0$, and $V(k)$ is decreasing and lower-bounded by 0. Then according to Lyapunov stability theory, it holds that $\lim_{k\to\infty} E_k = 0$, i.e., the joint error dynamic model (16) under the proposed MPC algorithm is stable at zero subject to the constraints, and the actual timetable will converge to the nominal timetable. The proof is complete. □

The result in Theorem 3.1 indicates the proposed MPC algorithm ensures the stability of the joint train traffic system without disturbances, which means that when the disturbances for the train regulation system disappear, the train traffic system converges to a stable state, which guarantees a good performance for the train regulation system. With the assumption of the observability, the considered metro line system is stable under the proposed MPC algorithm, which also reveals the controllability of the considered metro line system. Moreover, it should be noted that since the proposed MPC algorithm is based on state-feedback information, which allows the train to effectively adjust its speed as time evolves, and thus it is robust to uncertainty and disturbances. In addition, the considered objective function in this study takes a positive definite quadratic form. Thus the corresponding value function is also positive definite, which can be adopted as a Lyapunov function. If we change the control criteria to minimize the maximum span, the corresponding objective function of the formulated optimization problem will be changed, which may not be a positive definite quadratic form. Under this case, the value function of the optimization problem may not be employed as a Lyapunov function for establishing a stability condition. The stability analysis will become more difficult, which may resort to other methods for stability analysis.

4. Numerical examples

In this section, to demonstrate the performance of the proposed joint optimal dynamic train regulation and passenger flow control strategy for metro lines, we apply our proposed model and method to the actual Beijing metro line 9 that consists of 13 stations (i.e., $N = 12$) through three traffic scenarios. Beijing metro line 9 is a busy metro line including the largest railway station of Beijing (Beijing West Railway) and six transfer stations. During the peak hours of the day, the passenger flow in many stations is extremely large, which makes the arriving train usually overloaded and largely affects

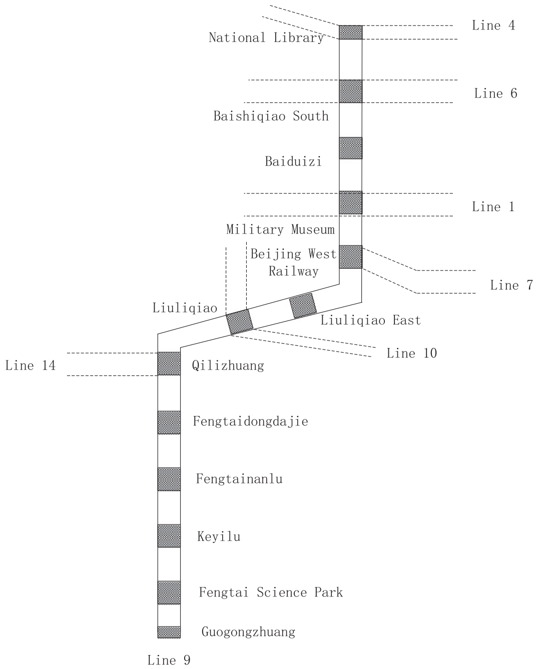

Fig. 6. Beijing metro line 9 map.

the operational efficiency and also leads to a safety hazard for the metro line system. Thus, it is necessary to design a joint dynamic train regulation and passenger flow control strategy to manage the entire metro line system, for improving the headway regularity and commercial speed under uncertain disturbances.

The map of the Beijing metro line 9 is shown in Fig. 6. We consider the single direction of line 9 from station Guogongzhuang to station National Library. The delay rate α is given as 0.02. The considered time step horizon is $T = 20$, the prediction step horizon is chosen as $M = 3$ and the scheduled headway is $H = 180$ s. The minimum allowable safety headway $t_{\min} = 160$ s, and we have $H - t_{\min} = 20$ s. The maximum capacity of the train for passengers $l_{\max} = 2000$, and we assume that $l_{\max} - L_j^i \leq 50$. The control constraints for the control force of the timetable are set as $u_{\min} = -20$ and $u_{\max} = 25$, which means that the increase of the adjusting running time and dwell time is not allowed to exceed 25 s and the decrease is not to exceed 20 s, and the control constraints for the control force of the passenger flow are set as $p_{\min} = -30$ and $p_{\max} = 0$, i.e., the decrease the adjusting passengers is not to exceed 30. In scenario 1, we compare our proposed method with other control policies in which the system parameters are considered as constant, to illustrate the benefit of our proposed joint dynamic control strategy for improving the headway regularity and commercial speed of metro lines. In scenario 2, we design the joint dynamic control strategy for the metro line with changing system parameters, and in scenario 3, we investigate the effect of the different weights in the cost function for improving the headway regularity and commercial speed. We choose the operating condition of the metro system during the morning peak hours from 7:00 am to 9:00 am. The QP formulation defined in (28) is solved by using the quadprog function from the MATLAB optimization tool box in each step of the simulation to find the optimal value as the joint optimal dynamic train regulation and passenger flow control strategy for metro lines.

4.1. Scenario 1: comparison with other control polices

To valid the effectiveness of the proposed joint optimal dynamic train regulation and passenger flow control strategy in this study, we compare it to the case with $\bar{u}_j^i = 0$ and the case with a traditional dynamic programming (DP) policy, respectively.

The system parameters and initial conditions are presented in Tables 3 and 4, respectively. The system parameters in each station are assumed to be constant. The passenger arrival rate γ_{j+1}^i for the busy station (such as a transfer station) is normally larger than that of nontransfer stations, and the coefficient β_{j+1}^i of the proportionality factor for exiting passengers for the transfer station is bigger than that of nontransfer stations. These values of the system parameters given in Table 3 for each station are different, which are based on the actual operating conditions of each station on metro line 9. The initial stage is chosen from time 7:00 am, and Table 4 shows that the maximum delay for the train is 35 s, and the maximum number of overloaded passengers is 40, both of which exceed the maximum adjustment values for the timetable and the passenger load capacity. Therefore the affected trains need several stations to compensate for the delays, and a

Table 3
The system parameters for each station.

Station	Index j	β_j^i	γ_j^i
Guogongzhuang	1	null	0.3
Fengtai Science Park	2	0.01	0.3
Keyilu	3	0.01	0.3
Fengtainanlu	4	0.01	0.3
Fengtaidongdajie	5	0.01	0.3
Qilizhuang	6	0.02	0.4
Liuliqiao	7	0.1	0.5
Liuliqiao East	8	0.02	0.3
Beijing West Railway	9	0.08	0.8
Militrary Museum	10	0.1	0.6
Baiduizi	11	0.02	0.3
Baishiqiao South	12	0.2	0.3
National Library	13	1	null

Table 4
The initial conditions for the deviations of timetable and passenger load at each station.

Station	1	2	3	4	5	6	7	8	9	10	11	12
Timetable	0	0	0	0	20	20	35	20	20	0	0	0
Passenger load	0	0	5	6	40	40	40	30	30	10	0	0

transient period is needed to reach the nominal timetable. In addition, without loss of generality, the weighted parameters for the cost function (18) are set to be the same, where $P = \text{diag}\{0.1, 0.1, \dots, 0.1\}$, $Q = \text{diag}\{0.1, 0, 0.1, 0 \dots, 0.1, 0\}$, and $R = \text{diag}\{0.1, 0.1, \dots, 0.1\}$, which means that the requirement for the reduced delays, the headway deviation, and the control force are the same. At stage $k = 10$, we assume that the trains are affected by an uncertain disturbance w_{10}, which is given as $w_{10} = (0, 0, 0, 0, 10, 10, 28, 10, 10, 0, 0, 0)$.

Under the above system parameters and initial conditions, at first we compare the proposed method to the case with $\bar{u}_j^i = 0$. For the initial delays of the trains, based on the proposed joint dynamic train regulation and passenger flow control model (16), and applying the proposed MPC Algorithm 3.1 to solve the optimization control problem (25), we can calculate the corresponding joint optimal dynamic train regulation and passenger flow control strategy. Let $\bar{x}1$ and $\bar{l}1$ be the train delay and the passenger load error without train regulation, i.e., $\bar{u}_j^i = 0$, respectively, and let $\bar{x}2$ and $\bar{l}2$ be the train delay and the passenger load error of the train under the proposed joint optimal control strategy, respectively. The notations of $\bar{x}1$ and $\bar{x}2$ are only used to denote the train delays. Let u and p be the control forces of the train timetable and the passenger load, respectively. The comparison results of the metro line under the case with the proposed joint optimal control strategy and the case with $\bar{u}_j^i = 0$ from station 6 to station 9 are summarised in Table 5. From Table 5, we can observe that the train delay $\bar{x}1$ is propagated from one train to the next train at stations 6–9 without train regulation, which overloads the trains. Meanwhile, the overloaded passenger flow leads to train delays. By comparison, under the proposed joint optimal control strategy, the train delay $\bar{x}2$ is effectively reduced and recovered to zero after two or three stages, and the transient period for recovering from the delays is short, and meanwhile the passenger load error of the train is also quickly reduced and converges to the nominal level after three stages. In addition, from Table 5, we can find that under $\bar{u}_j^i = 0$, the train delay $\bar{x}1$ lasts for about three to five stages for stations 6–9 and the corresponding values of the train delays are from 20 s to 35 s, while the control force u for the train timetable only needs two stages for recovering from the delays at stations 6–9 and the values of the control force u are less than the train delay value $\bar{x}1$, which shows that the joint optimal control strategy improves the efficiency for the metro lines recovering from disturbed situations.

Next, we compare the proposed joint optimal control policy with another train regulation method using dynamic programming (DP) for which the optimal decision is obtained by an one-time optimization (Lin and Sheu, 2010). The state variable considered in Lin and Sheu, 2010 is only the departure time of the train, which does not consider the dynamics of the passenger load of the trains, and the control variable is only the train running time and dwell time adjustment. The simulation results of the time deviations of the trains at stations 6–9 under the proposed method are plotted in Fig. 7(a). From Fig. 7(a), we can observe that the train delays for all the stations are effectively reduced along the following stages. Specially, at stage 4, the train delays are reduced to zero and the trains are operating according to the nominal timetable, and the full timetable recovery is achieved, which indicates the stability of the metro line system under the proposed method. Moreover, at stage 10, when the trains are affected by the uncertain disturbance that further leads to delays of the trains, the joint optimal control strategy can be calculated in real-time according to the current disturbance, and under the new joint optimal control strategy, the delays of the trains are reduced along the stages, and are all stabilized to zero after a few stages. In addition, the errors of passenger load at the different stages under the joint optimal control strategy are plotted in Fig. 7(b), which shows that the errors of passenger load are reduced along the stages and kept at zero at stage 4, which ensures that the passenger load of the trains are kept at a reasonable level. Additionally, the headway deviations for the

Table 5
The comparison results of the metro line from station 6 to station 9.

	Stage	1	2	3	4	5	6	7	8	9
	$\bar{x}1$	20	20	0	0	0	0	0	0	0
	$\bar{x}2$	20	5	0	0	0	0	0	0	0
Station 6	$\bar{l}1$	40	39	−8	5	0	0	0	0	0
	$\bar{l}2$	40	14	0	0	0	0	0	0	0
	u	−15	0	0	0	0	0	0	0	0
	p	−19	0	0	0	0	0	0	0	0
	$\bar{x}1$	35	20	20	0	0	0	0	0	0
	$\bar{x}2$	35	15	0	0	0	0	0	0	0
Station 7	$\bar{l}1$	40	28	35	−18	5	0	0	0	0
	$\bar{l}2$	40	11	3	0	0	0	0	0	0
	u	−5	−3	0	0	0	0	0	0	0
	p	−15	−3	0	0	0	0	0	0	0
	$\bar{x}1$	20	35	20	20	0	0	0	0	0
	$\bar{x}2$	20	15	4	0	0	0	0	0	0
Station 8	$\bar{l}1$	30	44	23	35	−24	5	0	0	0
	$\bar{l}2$	30	15	3	0	0	0	0	0	0
	u	−20	−11	0	0	0	0	0	0	0
	p	−22	−4	0	0	0	0	0	0	0
	$\bar{x}1$	20	20	35	20	20	0	0	0	0
	$\bar{x}2$	20	6	3	0	0	0	0	0	0
Station 9	$\bar{l}1$	30	28	53	9	32	−39	5	0	0
	$\bar{l}2$	30	7	5	0	0	0	0	0	0
	u	−14	−11	−3	0	0	0	0	0	0
	p	−10	−7	0	0	0	0	0	0	0

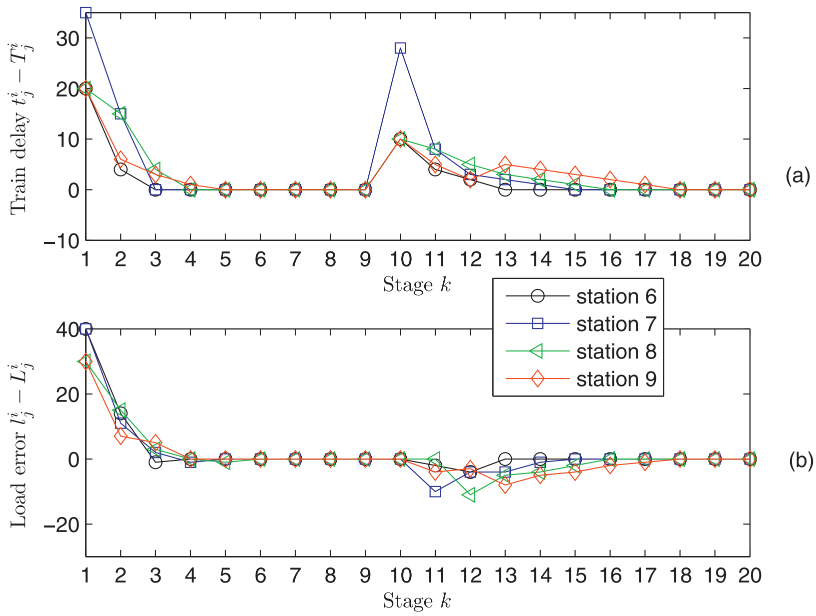

Fig. 7. The train delay and passenger load error at different stages under the MPC algorithm.

trains under the joint optimal control at stations 6–9 are plotted in Fig. 8, which shows that when the disturbance happens, there are fluctuations for the headway deviations from the nominal headway, and then the headway deviations converge to zero, i.e., the actual headway is kept at the nominal state and the headway regularity is improved. The headway regularity of the metro line reduces the average waiting time for the passengers. The optimal control forces for the train timetable and the passenger flow are plotted in Fig. 9(a) and (b), respectively, which shows that all the control forces satisfy the control constraints. In the end, according to the quadprog function from MATLAB optimization tool box, the optimization objective value is calculated as $J = 2080.4$. At each decision step, the computational time is only 2.71 s on a personal computer with four CPUs and 4.00GB computer memory, which shows that the proposed MPC algorithm can be implemented for practical metro lines in real-time.

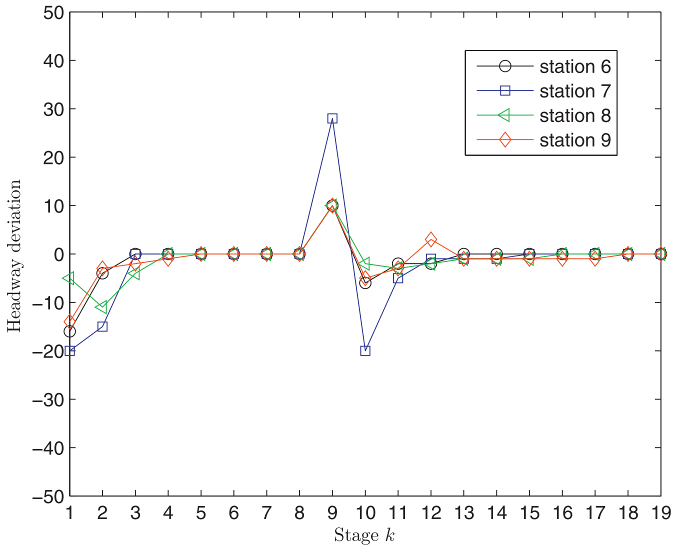

Fig. 8. The headway deviations at different stages under the MPC algorithm.

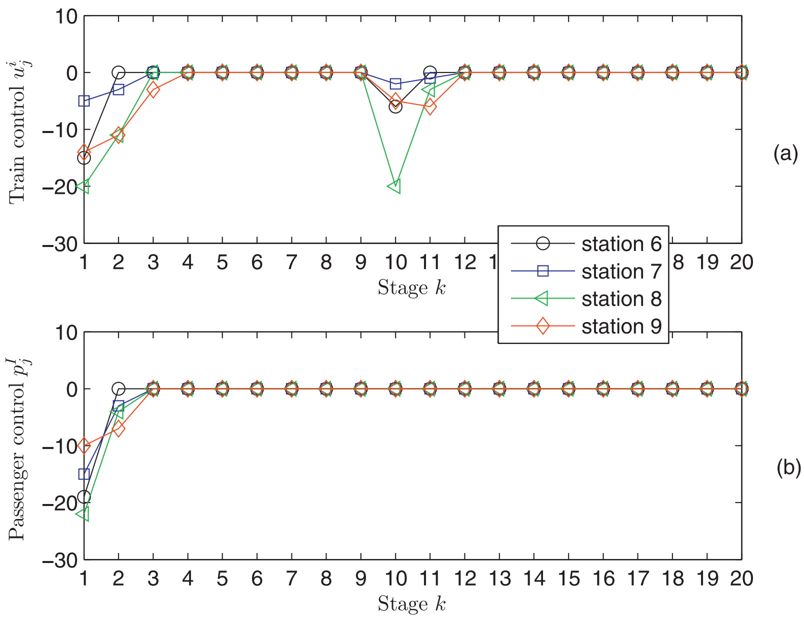

Fig. 9. The control forces at different stages.

The dynamic programming form for the proposed optimal control problem (25) is described by the Bellman equation $J_k^* = \min_{U_k}(E_k^T PE_k + (E_k - E_{k-1})^T Q(E_k - E_{k-1}) + U_k^T RU_k + J_{k+1}^*(E_{k+1}))$ and $U_k^* = \arg\min_{U_k}(E_k^T PE_k + (E_k - E_{k-1})^T Q(E_k - E_{k-1}) + U_k^T RU_k + J_{k+1}^*(E_{k+1}))$, subject to the state and control constraints in (25), where $J_k = \sum_{i=k}^{j_f}(E_i^T PE_i + (E_i - E_{i-1})^T Q(E_i - E_{i-1}) + U_i^T RU_i)$. By solving the joint train regulation and passenger flow control problem by the DP method, we can obtain the optimization solution for the train regulation and passenger flow control. Under the DP method, the time deviations of the trains and the errors of passenger loads at stations 6–9 are plotted in Fig. 10(a) and (b), respectively. By comparing Figs. 7(a) and 10(a), we can observe that the time delays are recovered from stage 7 under the DP policy, which is slower than the proposed MPC algorithm from stage 4, which means that the dynamic renewal optimization characteristic of the MPC algorithm is superior than the one time optimization of DP. Moreover, at stage 10 when the disturbance happens, the deviations of the train timetable under the DP policy have a larger fluctuation from stage 10 to stage 15 than that under the proposed MPC algorithm. Real-time control of the MPC algorithm has more robustness than the DP policy. In addition, according to Figs. 7(b) and 10(b), we can see that the fluctuation of the error for the passenger load under the DP method is bigger

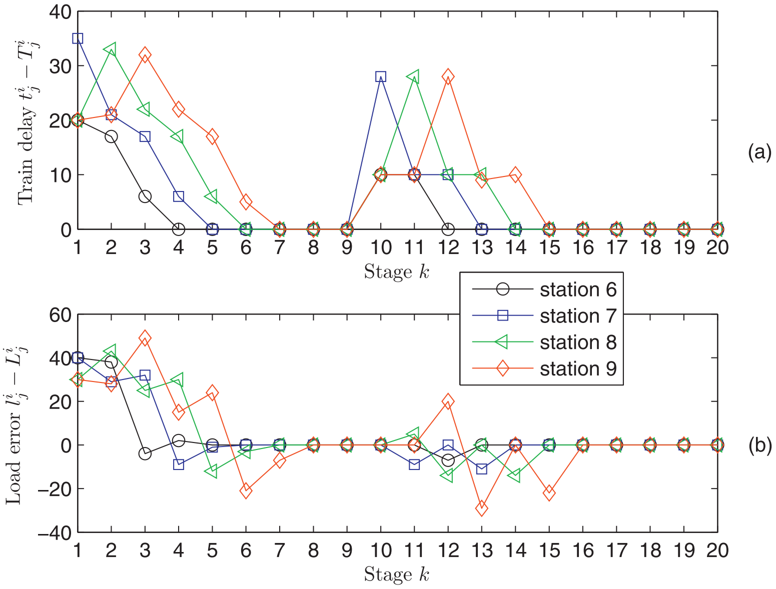

Fig. 10. The train delays and passenger load errors at different stages under the DP policy.

Table 6
The changing system parameters of the passengers arrival rates.

Index j	1	2	3	4	5	6	7	8	9	10	11	12
$k = 1:4$	0.4	0.4	0.4	0.4	0.4	0.5	0.6	0.4	0.7	0.6	0.4	0.4
$k = 5:8$	0.5	0.5	0.5	0.5	0.5	0.6	0.7	0.5	0.8	0.7	0.5	0.5
$k = 9:12$	0.6	0.6	0.6	0.6	0.6	0.7	0.8	0.6	0.9	0.8	0.6	0.6
$k = 13:16$	0.5	0.5	0.5	0.5	0.5	0.6	0.7	0.5	0.8	0.7	0.5	0.5
$k = 17:20$	0.4	0.4	0.4	0.4	0.4	0.5	0.6	0.4	0.7	0.6	0.4	0.4

than that under the MPC algorithm, which shows that the MPC algorithm can be effective to implement for controlling the overloaded passenger flow. Furthermore, by calculation, the optimization objective value based on the DP policy is obtained as $J = 8269.7$, which is larger than that based on the MPC algorithm. In the end, it should be noted that the large prediction errors will negatively affect the optimization performance. To avoid the large prediction errors, we usually chose a prediction horizon M in a short time for the proposed MPC method. With the short prediction horizon, any forecast errors are local and have limited impact since they will always be corrected by real-time data at the next interval.

4.2. Scenario 2: the general case with real-time updated system parameters

The system parameters for most actual metro lines change over time, such as the passenger arrival rates, so an actual metro line system is a time-varying system, and the corresponding control strategy needs to be made in real-time according to the updated information of the system parameters. However, the traditional dynamic programming method is hard to deal with this general case with real-time updated system parameters. In scenario 2, we consider this more general case and design the joint dynamic train regulation and passenger flow control strategy for metro lines with real-time updated system parameters. In this case we assume that at stages $k = 5$, $k = 9$ and $k = 13$, the trains are affected by uncertain disturbances, which are give as $w_5 = (0, 0, 0, 0, 45, 45, 55, 45, 40, 0, 0, 0)$, $w_9 = (0, 0, 0, 0, 25, 25, 25, 25, 0, 0, 0, 0)$ and $w_{13} = (0, 0, 0, 0, 10, 10, 0, 25, 10, 0, 0, 0)$. We next experiment with real-time updated parameters of the passenger arrival rate γ_{j+1}^i, which is shown in Table 6, where the passenger arrival rate has an increasing trend from stage $k = 1$ to $k = 8$, and reaches its maximum value from stage $k = 9$ to $k = 12$, and then has a decreasing trend from stage $k = 13$ to $k = 20$. Moreover, the passenger arrival rate γ_{j+1}^i is plotted in Fig. 11, which clearly shows the time-dependent passenger arrival flow. In addition, the coefficient β_{j+1}^i is the same to that in Scenario 1.

First, when the train regulation is not applied to the metro line system, the headway deviations for the trains at stations 6–9 is plotted in Fig. 12(a), which shows that the disturbances lead to a large fluctuation of the headway deviations of the trains from the nominal state, and negatively affects the waiting time of the passengers. The errors of passenger load are plotted in Fig. 12(b), which indicates that the passenger load also has large fluctuations from the nominal state. Because of the multiple times of the disturbances to the train delays, the headway deviations of the trains at stations and the

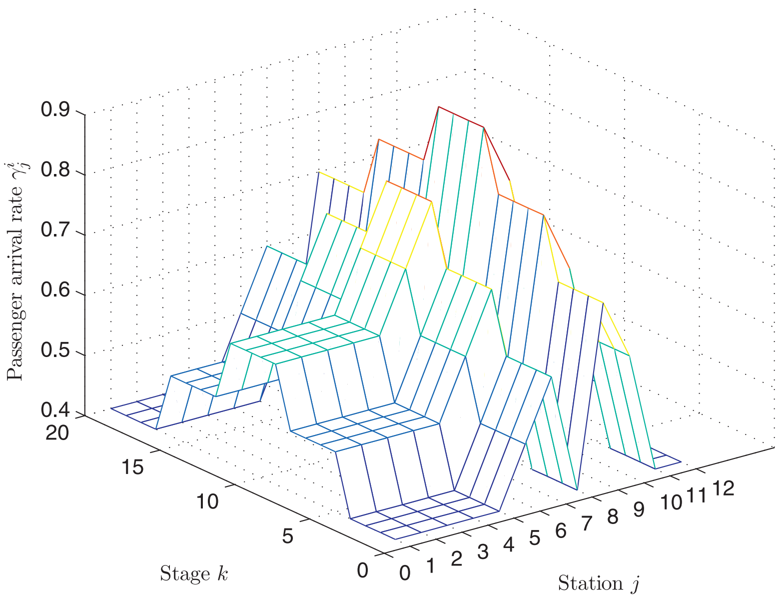

Fig. 11. The updated parameters of the passenger arrival rate.

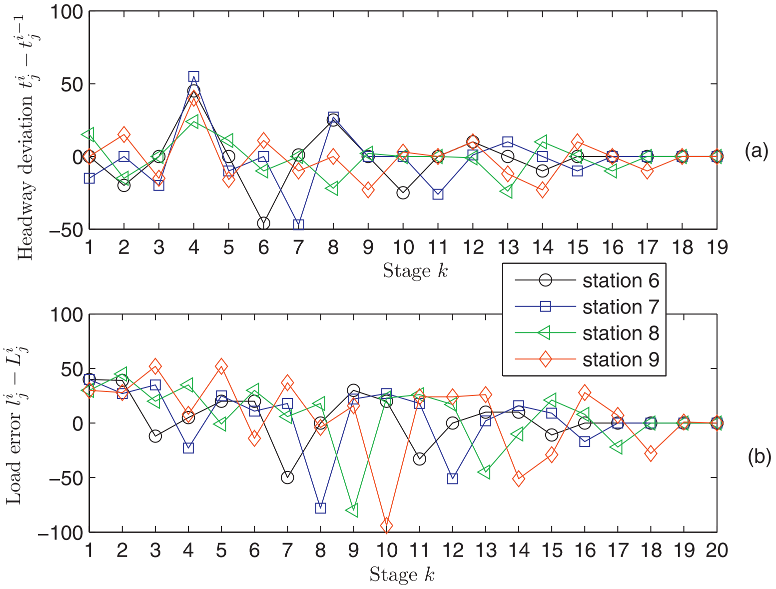

Fig. 12. The headway deviations and passenger load errors of the metro line without train regulation.

errors of passenger load have multiple fluctuations. The fluctuations of the headway deviations and the passenger load error negatively reduce the train operational efficiency and passenger service level.

According to the real-time updated parameter information and solving the optimal control problem (25) using Algorithm 3.1, the simulation results of the headway deviations at stations 6–9 are plotted in Fig. 13(a), and the errors of the passenger load at the different stages are plotted in Fig. 13(b). When a disturbance happens, the headway deviations of the trains at the stations and the errors of the passenger load are effectively reduced under the proposed joint optimal control strategy. For example, at stage 5, when the disturbance w_5 happens, it leads to the delays of the trains and fluctuations of the passenger load. Under the optimal joint control strategy, the delays of the trains and the fluctuations of the passenger load are effectively reduced and stabilized to about zero at stage 7. Similarly, when the disturbances w_9 and w_{13} happen, the delays of the trains and the fluctuations of the passenger load are all effectively reduced. In particular, when the disturbances disappear after stage 15, the delays of the trains and the fluctuations of the passenger load are stabilized at the stationary state (zero), i.e., the disturbed traffic is recovered to an acceptable situation. This shows the robustness and stability of the proposed joint train regulation and passenger flow control strategy.

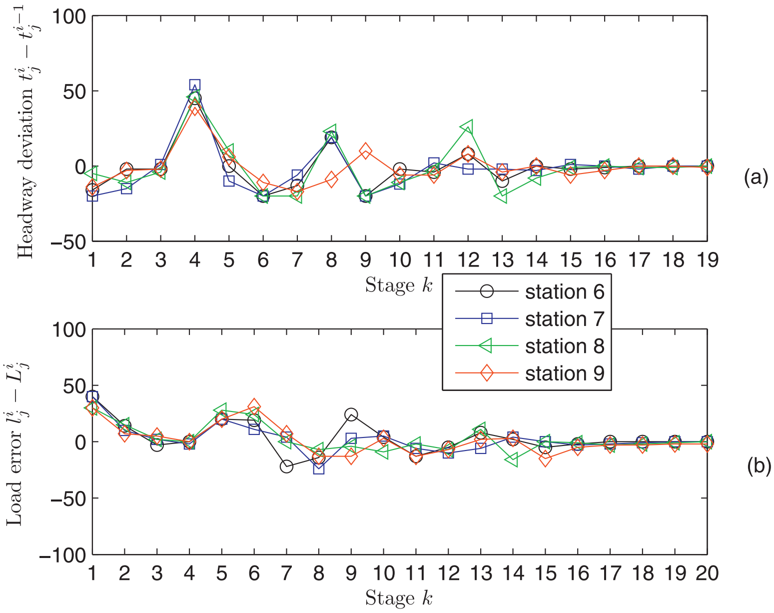

Fig. 13. The headway deviations and passenger load errors under the joint optimal control strategy.

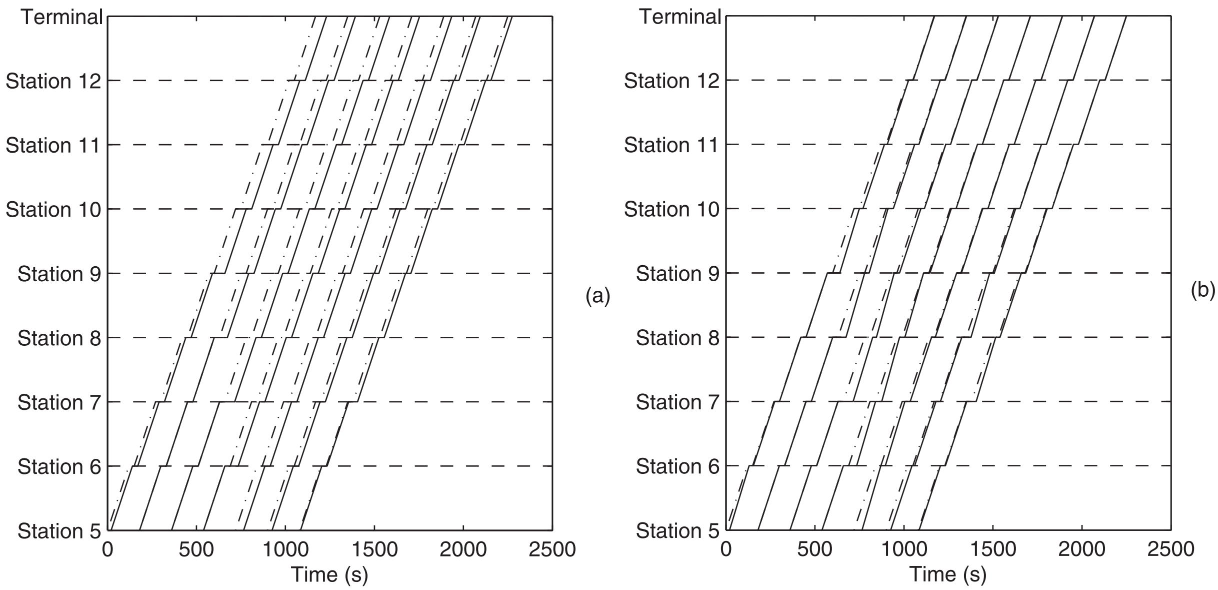

Fig. 14. The timetables of the metro line without train regulation (a) and with train regulation (b).

Moreover, the timetables for the metro line without train regulation and with train regulation are plotted in Fig. 14 (a) and (b), respectively, where the dotted lines represent the nominal timetable and the solid lines denote the actual timetable under disturbances. By comparison, we can see when a disturbance happens, the delays are propagated from one station to the next one under the case without train regulation, while under the optimal joint control strategy, the delays of the trains are effectively reduced and recovered from the disturbances to the nominal timetable in a short amount of time.

4.3. Scenario 3: different weights for headway regularity and commercial speed

In scenario 3, we investigate the effect of the different weights in the cost function (18) for improving the headway regularity and commercial speed. For the cost function (18), the first term denotes the errors for the timetable, and the minimization of the first term means to improve the commercial speed of the metro line, while the second term is related to the headway deviation of the trains, and the minimization of the second term means to improve the headway regularity

Table 7
The minimization timetable deviations and headway deviations for a set of different weights.

	(b, q)	Case 1 (0.01, 0.99)	Case 2 (0.04, 0.96)	Case 3 (0.08, 0.92)	Case 4 (0.10, 0.90)	Case 5 (0.50, 0.50)
Timetable Deviations	Station 5	27.9	24.3	23.3	23.1	22.9
	Station 6	40.7	33.2	30.1	29.2	26.6
	Station 7	96.5	92.9	92.6	92.2	92.1
	Station 8	66.6	59.3	58.2	57.8	57.4
	Station 9	56.4	45.4	43.1	42.6	40.9
Headway Deviations	Station 5	16.9	21.2	22.6	23.3	24.9
	Station 6	20.9	21.0	22.3	23.5	26.1
	Station 7	61.8	62.8	63.8	64.0	64.2
	Station 8	33.6	36.7	37.7	38.1	39.6
	Station 9	14.2	16.8	17.8	18.3	25.2

of the metro line, irrespective of the nominal timetable. So by adjusting the different weights in the cost function, we can realise a tradeoff between the headway regularity and commercial speed. In this scenario, the initial state for the deviations of the actual departure time is given as (0, 0, 0, 0, 20, 20, 60, 20, 20, 0, 0, 0), which means that at the initial stage, the train at station 7 is delayed by 60 s. Meanwhile, the initial state of the error passenger load is given as (0, 0, 5, 6, 40, 40, 40, 30, 30, 10, 0, 0). In addition, we assume that at stages $k = 5$ and $k = 9$, the trains are affected by uncertain disturbances, which are give as $w_5 = (0, 0, 0, 0, 10, 15, 25, 10, 10, 0, 0, 0)$ and $w_9 = (0, 0, 0, 0, 5, 5, 40, 10, 10, 0, 0, 0)$. The system parameters and the constraints conditions are the same to those of Scenario 1.

To investigate the effects of the different weights in the cost function for improving the headway regularity and commercial speed, we consider five cases of the metro line system with different weights in the cost function. The weighted parameters P and Q for the cost function (18) are set to be $P = \mathrm{diag}\{b, b, \ldots, b\}$ and $Q = \mathrm{diag}\{q, 0, q, 0 \ldots, q, 0\}$. Then the five cases are given in Table 7, where the weights for the timetable deviations are increasing from Case 1 to Case 5, and meanwhile the weights for the headway deviations are decreasing from Case 1 to Case 5. Define the sum of the timetable deviations at each station j for all the trains as $(\sum_i e_j^i e_j^i)^{\frac{1}{2}}$ and the sum of headway deviations at each station j for all the trains as $(\sum_i (e_j^i - e_j^{i-1})(e_j^i - e_j^{i-1}))^{\frac{1}{2}}$. Then the minimization timetable deviations and headway deviations for the different weights under Cases 1–5 for stations 5–9 are calculated in Table 7. From Table 7, we can observe that at station 7, the timetable deviations and headway deviations are both largest since the initial delay at station 7 is the biggest. With increasing weights for the timetable deviations, the timetable deviations are reduced from Case 1 to Case 5 for the trains at stations 5–9, which means that the increase of the weights for the timetable deviations improves the commercial speed of the metro line under delays. With decreasing weights for the headway deviations, the headway deviations are increased from Case 1 to Case 5 for the trains at stations 5–9, which indicates that the decreasing of the weights for the headway deviations reduces the headway regularity of the metro line system. Therefore, according to the results in Table 7, we can choose a proper set of weights of the cost function (18) for the timetable and headway deviations to realize a trade-off between the headway regularity and commercial speed for metro lines.

5. Conclusion

In this paper, the joint optimal dynamic train regulation and passenger flow control strategy was investigated to improve the headway regularity and commercial speed for metro lines. A coupled dynamic model for the evolution of the departure time and the passenger load of each train travelling on the metro line was constructed. By considering the headway regularity and commercial speed in the cost function, an optimal control problem for the joint dynamic train regulation and passenger flow control strategy was developed, which was solved by applying the model predictive control (MPC) algorithm, under which an optimal control law for the joint dynamic train regulation and passenger flow control strategy can be numerically calculated by efficiently solving a set of quadratic programming problems.

The proposed method provides a real-time train regulation and passenger flow control strategy in the form of a closed loop system, which can be effectively and quickly implemented for actual metro lines in real-time. Numerical examples show that, under the proposed joint optimal control strategy, the train delays, the passenger load errors and the train headway deviations are significantly reduced, and the train operational efficiency and passenger service level are improved.

It is worthy to mention that the proposed method is applicable to train delays in a certain range, and the research scope is a full timetable recovery from the train delays. For significantly larger delays, a new reference timetable should be designed, which is related to another rescheduling problem. Additionally, the joint optimal dynamic train regulation and passenger flow control strategy that considers the energy consumption is also an interesting issue and should be investigated in the future.

Acknowledgements

This work was supported by the National Natural Science Foundation of China (Nos. 71401007, 71422002, 71621001), and the Research Foundation of State Key Laboratory of Rail Traffic Control and Safety, Beijing Jiaotong University (No. RCS2016ZJ002). The work of Maged Dessouky was partially based on support by Metrans and the Volvo Research and Education Foundation.

Appendix A. Derivation of (11)

The first equation of (10) can be rewritten as

$$\begin{aligned} t^i_{j+1} &= \frac{1}{1-\alpha\gamma^i_{j+1}}t^i_j - \frac{\alpha\gamma^i_{j+1}}{1-\alpha\gamma^i_{j+1}}t^{i-1}_{j+1} + \frac{\alpha\beta^i_{j+1}}{1-\alpha\gamma^i_{j+1}}l^i_j + \frac{\alpha}{1-\alpha\gamma^i_{j+1}}p^i_{j+1} + \frac{1}{1-\alpha\gamma^i_{j+1}}D_{j+1} \\ &+ \frac{1}{1-\alpha\gamma^i_{j+1}}R^i_j + \frac{1}{1-\alpha\gamma^i_{j+1}}u^i_j + \frac{1}{1-\alpha\gamma^i_{j+1}}t^i_j w^i_j. \end{aligned} \tag{32}$$

Then, by substituting (32) into the second equation of (10), we can get that the second equation of (10) is equivalent to

$$\begin{aligned} l^i_{j+1} &= (1-\beta^i_{j+1})l^i_j + \frac{\gamma^i_{j+1}}{1-\alpha\gamma^i_{j+1}}t^i_j - \left(\frac{\alpha\gamma^{i\;2}_{j+1}}{1-\alpha\gamma^i_{j+1}} + \gamma^i_{j+1}\right)t^{i-1}_{j+1} + \frac{\alpha\beta^i_{j+1}\gamma^i_{j+1}}{1-\alpha\gamma^i_{j+1}}l^i_j + \frac{\alpha\gamma^i_{j+1}}{1-\alpha\gamma^i_{j+1}}p^i_{j+1} \\ &+ \frac{\gamma^i_{j+1}}{1-\alpha\gamma^i_{j+1}}D_{j+1} + \frac{\gamma^i_{j+1}}{1-\alpha\gamma^i_{j+1}}R^i_j + \frac{\gamma^i_{j+1}}{1-\alpha\gamma^i_{j+1}}u^i_j + \frac{\gamma^i_{j+1}}{1-\alpha\gamma^i_{j+1}}t^i_j w^i_j + p^i_{j+1}, \end{aligned} \tag{33}$$

which can be further rewritten as

$$\begin{aligned} l^i_{j+1} &= (1-\beta^i_{j+1})l^i_j + \frac{\gamma^i_{j+1}}{1-\alpha\gamma^i_{j+1}}t^i_j - \left(\frac{\alpha\gamma^i_{j+1}}{1-\alpha\gamma^i_{j+1}}\right)t^{i-1}_{j+1} + \frac{\alpha\beta^i_{j+1}\gamma^i_{j+1}}{1-\alpha\gamma^i_{j+1}}l^i_j + \frac{\alpha\gamma^i_{j+1}}{1-\alpha\gamma^i_{j+1}}p^i_{j+1} \\ &+ \frac{\gamma^i_{j+1}}{1-\alpha\gamma^i_{j+1}}D_{j+1} + \frac{\gamma^i_{j+1}}{1-\alpha\gamma^i_{j+1}}R^i_j + \frac{\gamma^i_{j+1}}{1-\alpha\gamma^i_{j+1}}u^i_j + \frac{\gamma^i_{j+1}}{1-\alpha\gamma^i_{j+1}}t^i_j w^i_j + p^i_{j+1}. \end{aligned} \tag{34}$$

For $x^i_j = [t^i_j, l^i_j]^T$ and $\bar{u}^i_j = [u^i_j, p^i_{j+1}]^T$, by collecting terms for (32) and (34), it can be easily obtained that

$$x^i_{j+1} = A^i_j x^i_j + B^i_j x^{i-1}_{j+1} + C^i_j \bar{u}^i_j + G^i_j (D_{j+1} + R^i_j + w^i_j).$$

where $A^i_j = \begin{bmatrix} \frac{1}{1-\alpha\gamma^i_{j+1}} & \frac{\alpha\beta^i_{j+1}}{1-\alpha\gamma^i_{j+1}} \\ \frac{\gamma^i_{j+1}}{1-\alpha\gamma^i_{j+1}} & 1-\beta^i_{j+1} + \frac{\alpha\gamma^i_{j+1}\beta^i_{j+1}}{1-\alpha\gamma^i_{j+1}} \end{bmatrix}$, $B^i_j = \begin{bmatrix} \frac{-\alpha\gamma^i_{j+1}}{1-\alpha\gamma^i_{j+1}} & 0 \\ \frac{-\gamma^i_{j+1}}{1-\alpha\gamma^i_{j+1}} & 0 \end{bmatrix}$, $C^i_j = \begin{bmatrix} \frac{1}{1-\alpha\gamma^i_{j+1}} & \frac{\alpha}{1-\alpha\gamma^i_{j+1}} \\ \frac{\gamma^i_{j+1}}{1-\alpha\gamma^i_{j+1}} & \frac{1}{1-\alpha\gamma^i_{j+1}} \end{bmatrix}$, $G^i_j = \begin{bmatrix} \frac{1}{1-\alpha\gamma^i_{j+1}} \\ \frac{\gamma^i_{j+1}}{1-\alpha\gamma^i_{j+1}} \end{bmatrix}$.

Appendix B. Derivation of (14)

Subtracting (12) from the first equation of (10) gives that

$$(t^i_{j+1} - T^i_{j+1}) = (t^i_j - T^i_{j+1}) + \alpha(\gamma^i_{j+1}((t^i_{j+1} - T^i_{j+1}) - (t^{i-1}_{j+1} - T^{i-1}_{j+1})) + \beta^i_{j+1}(l^i_j - L^i_j) + p^i_{j+1}) + u^i_j + w^i_j. \tag{35}$$

Similarly, by subtracting (13) from the second equation of (10), one can get that

$$(l^i_{j+1} - L^i_{j+1}) = (l^i_j - L^i_j) + \gamma^i_{j+1}((t^i_{j+1} - T^i_{j+1}) - (t^{i-1}_{j+1} - T^{i-1}_{j+1})) - \beta^i_{j+1}(l^i_j - L^i_j) + p^i_{j+1}. \tag{36}$$

Then for $e^i_j = [t^i_j - T^i_j, l^i_j - L^i_j]^T$, similar to derivation process of (11), by collecting terms for (35) and (36), one can obtain that

$$e^i_{j+1} = A^i_j e^i_j + B^i_j e^{i-1}_{j+1} + C^i_j \bar{u}^i_j + G^i_j w^i_j.$$

where A^i_j, B^i_j, C^i_j, and G^i_j take the same forms in (11).

Appendix C. The definitions of matrices

$$\bar{A}_k = \begin{bmatrix} B_0^k & 0 & 0 & 0 & \cdots \\ A_1^{k-1} & B_1^{k-1} & 0 & 0 & \cdots \\ & \cdots & \cdots & \cdots & \\ 0 & \cdots & 0 & A_{N-1}^{k-N+1} & B_{N-1}^{k-N+1} \end{bmatrix}_{2N\times 2N}.$$

$$\bar{B}_k = \begin{bmatrix} C_0^k & 0 & 0 & \cdots \\ 0 & C_1^{k-1} & 0 & \cdots \\ & \cdots & \cdots & \cdots \\ 0 & \cdots & \cdots & C_{N-1}^{k-N+1} \end{bmatrix}_{2N\times 2N}.$$

$$\bar{G}_k = \begin{bmatrix} G_0^k & 0 & 0 & \cdots \\ 0 & G_1^{k-1} & 0 & \cdots \\ & \cdots & \cdots & \cdots \\ 0 & \cdots & \cdots & G_{N-1}^{k-N+1} \end{bmatrix}_{2N\times N}.$$

$$F = \begin{bmatrix} \bar{A}_k \\ \bar{A}_{k+1}\bar{A}_k \\ \cdots \\ \bar{A}_{k+M-1}\bar{A}_{k+M-2}\ldots\bar{A}_k \end{bmatrix}.$$

$$\Phi = \begin{bmatrix} \bar{B}_k & 0 & 0 & \cdots \\ \bar{A}_{k+1}\bar{B}_k & \bar{B}_{k+1} & 0 & \cdots \\ & \cdots & \cdots & \cdots \\ \bar{A}_{k+1}\bar{A}_{k+2}\ldots\bar{A}_{k+M-1}\bar{B}_k & \bar{A}_{k+2}\ldots\bar{A}_{k+M-1}\bar{B}_{k+1} & \cdots & \bar{B}_{k+M-1} \end{bmatrix}.$$

Appendix D. Derivation of (28) from (26)

For $E = [E_{k+1}^T, E_{k+2}^T, \ldots, E_{k+M}^T]^T$ and $U = [U_k^T, U_{k+1}^T, \ldots, U_{k+M-1}^T]^T$, the objective function for the optimization problem (26) can be rewritten as

$$E^T\bar{P}E + E^T\bar{Q}E + U^T\bar{R}U \tag{37}$$

where $\bar{P}$, $\bar{Q}$ and $\bar{R}$ can be directly obtained from the objective function of (26).

Then, by substituting $E = FE_k + \Phi U$ in the objective function (37), one can get that

$$\begin{aligned} &E^T\bar{P}E + E^T\bar{Q}E + U^T\bar{R}U \\ &= (FE_k + \Phi U)^T\bar{P}(FE_k + \Phi U) + (FE_k + \Phi U)^T\bar{Q}(FE_k + \Phi U) + U^T\bar{R}U \\ &= U^T(\Phi^T\bar{P}\Phi + \Phi^T\bar{Q}\Phi + \bar{R})U + 2U^T(\Phi^T\bar{P}FE_k + \Phi^T\bar{Q}FE_k) + F^T\bar{P}FE_k^2 + F^T\bar{Q}FE_k^2, \end{aligned} \tag{38}$$

which equals to the objective function of (28).

In addition, recalling that $E = [E_{k+1}^T, E_{k+2}^T, \ldots, E_{k+M}^T]^T$, the constraint $H_1(E_{k+j} - E_{k+j+1}) \le (H - t_{\min})I_{N\times 1}$, $j = 0, 1, \ldots, M-1$ in (26) can be rewritten to matrix form as

$$H_3H_4E + H_3H_5E_k \le (H - t_{\min})I_{MN\times 1}, \tag{39}$$

where H_3 is a matrix of $MN \times 2MN$ dimension, in which for each row i of the matrix, the element $H_3(i, 2i-1) = 1$, and all other elements for this row equal to zero,

$$H_4 = \begin{bmatrix} -I_{2N} & 0_{2N} & 0_{2N} & 0_{2N} & \cdots \\ I_{2N} & -I_{2N} & 0_{2N} & 0_{2N} & \cdots \\ & \cdots & \cdots & \cdots & \\ 0_{2N} & \cdots & 0_{2N} & I_{2N} & -I_{2N} \end{bmatrix}_{2MN\times 2MN}, \text{ and } H_5 = \begin{bmatrix} I_{2N} \\ 0_{2N} \\ \vdots \\ 0_{2N} \end{bmatrix}_{2MN\times 2N}.$$

By substituting $E = FE_k + \Phi U$ into the constraint (39), one can obtain that constraint (39) is equivalent to

$$H_3H_4\Phi U \le (H - t_{\min})I_{MN\times 1} - H_3H_4FE_k - H_3H_5E_k, \tag{40}$$

which corresponds to the first constraint in (28).

Similarly, one can obtain that the constraints $H_2E_{k+j+1} \leq L_{k+j+1}$, $U_{k+j} \leq U_{\max}$, and $-U_{k+j} \leq -U_{\min}$ $j = 0, 1, \ldots, M-1$ in (26) are equivalent to $H_6\Phi U \leq L - H_6FE_k$, $I_{2MN}U \leq \bar{U}_{\max}$, and $-I_{2MN}U \leq -\bar{U}_{\min}$, respectively, where H_6 is a matrix of $MN \times 2MN$ dimension, in which for each row i of the matrix, the element $H_6(i, 2i) = 1$, and all other elements for this row equal to zero, $L = [L^T_{k+1}, L^T_{k+2}, \ldots, L^T_{k+M}]^T$, $\bar{U}_{\max} = [U^T_{\max}, U^T_{\max}, \ldots, U^T_{\max}]^T_{2MN\times 1}$, and $\bar{U}_{\min} = [U^T_{\min}, U^T_{\min}, \ldots, U^T_{\min}]^T_{2MN\times 1}$, which corresponds to the other constraints in (28).

References

Abril, M., Barber, F., Ingolotti, L., Salido, M., Tormos, P., Lova, A., 2008. An assessment of railway capacity. Trans. Res. Part E 44 (5), 774–806.
Assis, W.O., Milani, B.E., 2004. Generation of optimal schedules for metro lines using model predictive control. Automatica 40 (8), 1397–1404.
Cacchiani, V., Huisman, D., Kidd, M., Kroon, L., Toth, P., Veelenturf, L., Wagenaar, J., 2014. An overview of recovery models and algorithms for real-time railway rescheduling. Trans. Res. Part B 63 (2), 15–37.
Caimi, G., Fuchsberger, M., Laumanns, M., Lthi, M., 2007. A model predictive control approach for discrete-time rescheduling in complex central railway station areas. Comput. Operat. Res. 27 (3), 145–155.
Campion, G., Van Breusegem, V., Pinson, P., Bastin, G., 1985. Traffic regulation of an underground railway transportation system by state feedback. Optimal Contr. Appl. Methods 6 (4), 385–402.
Chang, C., Thia, B., 1996. Online rescheduling of mass rapid transit systems: fuzzy expert system approach. IEE Proc. Elect. Power Appl. 143 (4), 307–316.
Chang, S.C., Chung, Y.C., 2005. From timetabling to train regulation–a new train operation model. Inf. Softw. Technol. 47 (9), 575–585.
Corman, F., D'Ariano, A., Pacciarelli, D., Pranzo, M., 2012. Optimal inter-area coordination of train rescheduling decisions. Trans. Res. Part E 48, 71–88.
Cury, J.E., Gomide, F.A.C., Mendes, M.J., 1980. A methodology for generation of optimal schedules for an underground railway system. IEEE Trans. Automat. Contr. 25 (2), 217–222.
Daganzo, C.F., 2009. A headway-based approach to eliminate bus bunching: systematic analysis and comparisons. Trans. Res. Part B 43, 913–921.
Daganzo, C.F., Pilachowski, J., 2011. Reducing bunching with bus-to-bus cooperation. Trans. Res. Part B. 45, 267–277.
Dundar, S., Sahin, I., 2013. Train re-scheduling with genetic algorithms and artificial neural networks for single-track railways. Trans. Res. Part C. 27, 1–15.
Eberlein, X.J., Wilson, N.H.M., Bernstein, D., 2001. The holding problem with real-time information available. Trans. Sci. 35 (1), 1–18.
Fernandez, A., Cucala, A., Vitoriano, B., de Cuadra, F., 2006. Predictive traffic regulation for metro loop lines based on quadratic programming. proceedings of the institution of mechanical engineers. Part F: J. Rail Rapid Transit 220 (2), 79–89.
Goodman, C., Murata, S., 2001. Metro traffic regulation from the passenger perspective. Proc. Ins. Mech. Eng. Part F: J. Rail Rapid Transit 215 (2), 137–147.
Das Gupta, S., Kevin Tobin, J., Pavel, L., 2016. A two-step linear programming model for energy-efficient timetables in metro railway networks. Trans. Res. Part B 93, 57–74.
Haddad, J., Ramezani, M., Geroliminis, N., 2013. Cooperative traffic control of a mixed network with two urban regions and a freeway. Trans. Res. Part B 54 (2), 17–36.
Kang, L., Wu, J., Sun, H., Zhu, X., Wang, B., 2015. A practical model for last train rescheduling with train delay in urban railway transit networks. Omega 50, 29–42.
Le, T., Hai, L.V., Nazarathy, Y., Bao, V., Hoogendoorn, S., 2013. Linear-quadratic model predictive control for urban traffic networks. Procedia-Social Behav. Sci. 80 (11), 512–530.
Li, S.K., De Schutter, B., Yang, L.X., Gao, Z.Y., 2016. Robust model predictive control for train regulation in underground railway transportation. IEEE Trans. Control Syst. Technol. 24 (3), 1075–1083.
Li, X., Hong, K.L., 2014. An energy-efficient scheduling and speed control approach for metro rail operations. Trans. Res. Part B 64 (4), 73–89.
Lin, S., De Schutter, B., Xi, Y., Hellendoorn, H., 2011. Fast model predictive control for urban road networks via milp. IEEE Trans. Intell. Transp. Syst. 12 (3), 846–856.
Lin, W., Sheu, J., 2010. Automatic train regulation for metro lines using dual heuristic dynamic programming. Proc. Ins. Mech. Eng. Part F: J. Rail Rapid Transit 224 (1), 15–23.
Mannino, C., Mascis, A., 2009. Optimal real-time traffic control in metro stations. Oper. Res. 57 (4), 1026–1039.
Mayne, D.Q., Rawlings, J.B., Rao, C.V., Scokaert, P.O.M., 2000. Constrained model predictive control: stability and optimality. Automatica 36, 789–814.
Minciardi, R., Paolucci, M., Presenti, R., 1995. Generating optimal schedules for an underground railway line. In: Proceedings of the 34th IEEE Conference on Decision and Control, pp. 4082–4085.
Niu, H., Zhou, X., 2013. Optimizing urban rail timetable under time-dependent demand and oversaturated conditions. Trans. Res. Part C 36 (11), 212–230.
Niu, H., Zhou, X., Gao, R., 2015. Train scheduling for minimizing passenger waiting time with time-dependent demand and skip-stop patterns: nonlinear integer programming models with linear constraints. Trans. Res. Part B 76, 117–135.
Sánchez-Martínez, G., Koutsopoulos, H., Wilson, N., 2016. Real-time holding control for high-frequency transit with dynamics. Trans. Res. Part B 83, 1–19.
Sheu, J.W., Lin, W.S., 2012. Energy-saving automatic train regulation using dual heuristic programming. IEEE Trans. Veh. Technol. 61 (4), 1503–1514.
Sun, L., Jin, J.G., Lee, D.H., Axhausen, K.W., Erath, A., 2014. Demand-driven timetable design for metro services. Trans. Res. Part C 46, 284–299.
Van Breusegem, V., Campion, G., Bastin, G., 1991. Traffic modeling and state feedback control for metro lines. IEEE Trans. Automat. Contr. 36 (7), 770–784.
Vansteenwegen, P., Oudheusden, D.V., 2004. Developing railway timetables which guarantee a better service. Eur. J. Oper. Res. 173 (1), 337–350.
Veelenturf, L., Kidd, M., Cacchiani, V., Kroon, L., Toth, P., 2016. A railway timetable rescheduling approach for handling large scale disruptions. Trans. Sci. 50 (3), 841–862.
Xu, X., Li, K., Yang, L., 2016. Rescheduling subway trains by a discrete event model considering service balance performance. Appl. Math. Model 40 (2), 1446–1466.
Yang, L.X., Zhang, Y., Li, S.K., Gao, Y., 2016. A two-stage stochastic integer programming model or the transfer activity choice in metro networks. Trans. Res. Part B 83, 271–297.
Yin, J., Tang, T., Yang, L., Gao, Z., Ran, B., 2016. Energy-efficient metro train rescheduling with uncertain time-variant passenger demands: an approximate dynamic programming approach. Trans. Res. Part B 91, 178–210.
Yin, J., Yang, L., Tang, T., Gao, Z., Ran, B., 2017. Dynamic passenger demand oriented metro train scheduling with energy-efficiency and waiting time minimization: mixed-integer linear programming approaches. Trans. Res. Part B 97, 182–213.